Kinematic Sickness: Understanding Cybersickness Through Body Kinematics

Carlos A. Tirado Cortes, Yiheng Chi, Juno Kim, Hsiang-Ting Chen

Fig. 1: Experiment setup.

Abstract—Postural Instability Theory (PIT) proposes that individuals who are naturally unstable on their feet are more susceptible to cybersickness. We hypothesize that this relationship extends to locomotive VR, such that people who exhibit greater instability when walking without VR will also be more susceptible to cybersickness in a locomotive VR setup. To test this, we analyzed participants' natural walking kinematics alongside their cybersickness responses and kinematic patterns during mobile VR use. Our results showed that vertical Center of Mass movement during pre-VR walking showed promise for identifying individuals susceptible to cybersickness. Spatial stability metrics emerged as stronger predictors of cybersickness than time-series measures, suggesting that spatial characteristics of gait may be more informative indicators of susceptibility in mobile VR contexts. These findings highlight the importance of accounting for baseline postural stability when designing and personalizing mobile VR experiences.

Index Terms—Cybersickness, Postural Instability, Center of Mass, Virtual Reality, Kinematic Analysis, Machine Learning

1 Introduction

The growth in popularity of virtual reality and the affordability of its tracking devices have made the use of body movements increasingly common for enhancing the user experience in current virtual environments. It has been theorized that full-body interaction will decrease the mismatch between the visual and vestibular systems, thereby reducing the conflict users experience during VR sessions [28], which, in turn, leads to a reduction in cybersickness symptoms [4, 44]. However, even in walking environments, users still experience symptoms of cybersickness [41], such as discomfort, headaches, or nausea [51].

The study of cybersickness has led to the development of multiple theories that describe the phenomenon and its causes [31]. Theories such as the sensory conflict theory [17, 20] and the postural instability theory [36] have been among the most prominent theories explaining the appearance of sickness in VR participants. A previous study hypothesized that, at least during mobile environments, postural instability theory is more relevant [52].

Postural instability theory (PIT) states that prolonged exposure to postural instability contributes to the generation of symptoms associated with motion sickness. One key proposal of PIT is that individuals who are naturally unstable on their feet will also be more susceptible to cybersickness [27, 32, 36, 46].

Studies analyzing postural instability have primarily recorded participants in non-locomotive contexts (standing or sitting), commonly measuring center of pressure (CoP) [7, 18, 27], though some have also employed motion capture of head and torso movements [47] or head tracking during active VR tasks [1]. These studies consistently find that spatial and temporal CoP characteristics differ between "Sick" and "Not Sick" groups, with postural instability detectable before users report any symptoms.

However, few studies have examined the relationship between pre-VR walking, VR walking, and cybersickness. Previous research has used non-VR walking as a baseline for kinematic [51] and physiological [52] measurements during VR experiments. Yet, none have systematically analyzed how baseline locomotion performance influences subsequent VR behavior. This gap represents an underexplored area in understanding how natural movement characteristics might

- *Carlos Tirado is with the Discipline of Design at the School of Architecture, Design and Planning, University of Sydney. E-mail: carlos.tiradocortes@sydney.edu.au.*
- *Yiheng Chi is with the School of Mathematical Sciences, Adelaide University. E-mail: chiyiheng268@gmail.com.*
- *Juno Kim is with the Sensory Process Research Laboratory at the University of New South Wales. E-mail: juno.kim@unsw.edu.au.*
- *Hsiang-Ting Chen is with the School of Computer Science and Information Technology, and the Australian Institute for Machine Learning, Adelaide University. E-mail: tim.chen@adelaide.edu.au.*

Manuscript received xx xxx. 201x; accepted xx xxx. 201x. Date of Publication xx xxx. 201x; date of current version xx xxx. 201x. For information on obtaining reprints of this article, please send e-mail to: reprints@ieee.org. Digital Object Identifier: xx.xxxx/TVCG.201x.xxxxxxx

predict responses during VR interaction.

1.1 Paper Contributions

This paper extends PIT to mobile VR by hypothesizing and showing that individuals with greater natural walking instability in non-VR conditions experience heightened susceptibility to cybersickness in mobile VR.

Our methods analyzed users' walking patterns before and during interaction with a VR walking scenario. We calculated the displacement in three directions: lateral, forward, and vertical, as well as the total magnitude of displacement of the center of mass from a *predicted path*. This displacement was calculated for both the Center of Mass (CoM) and the head movement.

We analyzed both the spatial and temporal characteristics of the multiple displacements of the CoM and head movement. We hypothesized that, similar to the non-locmotive experiments reported in previous works, we would observe differences in the No-VR portion of the experiment between the group that experienced cybersickness and the group that did not [43].

This paper makes multiple contributions. First, to the best of our knowledge, this is the first study to analyze participants' walking patterns before they enter VR and to draw conclusions about how they relate to the postural instability theory. We aim to analyze how natural walking data can help us understand the participants' developed cybersickness.

Second, we conducted a time-series analysis of walking patterns in users experiencing cybersickness, similar to previous postural instability studies [7, 27]. We contribute by analyzing the temporal dynamics of walking patterns to understand how sway evolves relative to cybersickness onset. Our methodological contribution includes the expected path methodology for measuring locomotion instability and its utility in establishing the relationship between movement deviation and cybersickness symptoms.

Finally, our third contribution seeks to understand which metrics contribute most to the development of cybersickness. To address this, we employed logistic regression to determine which of these metrics better identifies users who experience cybersickness and which displacement direction most strongly contributes to its onset.

2 Related Work

2.1 Non-Locomotive Baseline Measures

A subset of postural instability studies aims to understand the relationship between postural sway and symptoms associated with different types of sickness, like motion sickness or cybersickness. One of the most common methods is measuring participants' postural sway before exposure to visual stimuli that can trigger sickness symptoms [46]. These studies typically employ a paradigm in which participants' postural activity is recorded during non-locomotive tasks (such as standing or sitting) to measure their natural level of instability. Then interact with a virtual environment that induces cybersickness through visually induced motion. Later, researchers investigated the spatial and temporal parameters of the center of pressure (CoP) to understand movement patterns in both symptomatic and asymptomatic groups [42].

This approach has been widely adopted, with most contributions to postural instability theory employing similar methodologies [1,7,27,53]. These studies commonly analyze postural activity metrics including center of pressure measurements [1, 7, 27, 53] and motion-capture body segments [47] to understand postural instability and cybersickness. Work by Weech et al. [53] extended the pre-VR prediction approach, showing that balance measures accounted for 37% of the variance in cybersickness, though measurements remained limited to static standing.

Arcioni et al. [1] reported that anterior-posterior CoP variability was significantly greater in the "sick" group. Smart et al. [43] found that participants who became sick exhibited distinct postural sway patterns, specifically increases in magnitude and spatial complexity, but decreases in temporal complexity, compared to those who remained well. Building on this work, Munafo et al. [27] demonstrated that temporal dynamics differed between symptomatic and asymptomatic groups, but only under specific VR scenarios. Curry et al. [7] later corroborated these findings, concluding that task type influences whether temporal dynamics of body motion can identify postural instability.

Building on these non-locomotive postural assessments, our work contributes new insights by extending pre-VR cybersickness prediction to dynamic locomotion. While Weech et al. [53] established the predictive value of non-locomotive balance measures, to the best of our knowledge, this is the first study to analyze baseline walking data from participants in a natural (non-VR) environment prior to exposure to VR. Our work would be the first to calculate the No-VR spatial and temporal dynamics and compare them to their walking behavior within a VR environment. This approach enables us to investigate whether individuals who exhibit natural postural instability during baseline walking are more susceptible to cybersickness during VR walking, thereby extending the postural instability theory from non-locomotive tasks to locomotive environments.

2.2 Studying Cybersickness in Mobile Contexts

A 2018 review [28] noted that the area of cybersickness in VR walking environments is underexplored. However, existing studies primarily treat cybersickness as a secondary outcome measure rather than as the primary focus of investigation. Studies typically use quantification of cybersickness as a measure of the success or failure of their implementations [15, 24, 54], without examining the mechanisms underlying cybersickness itself.

Similarly, mobile VR experiments employ cybersickness as a benchmark to compare VR walking with alternative locomotion methods [22, 25, 40, 55]. These studies repeatedly demonstrate that participants experience minimal cybersickness during VR walking compared to other VR navigation techniques [40, 55], reinforcing preferences for room-scale interaction [25]. Yet despite this consistent finding that VR walking reduces cybersickness, researchers have not examined the underlying walking characteristics that contribute to this advantage.

There have been very few projects that have studied cybersickness as a primary research objective in mobile VR contexts. The work by Setu et al. [41] investigated the relationship between physiological signals, cognitive load, and cybersickness during VR walking. This finding corroborates earlier work [52] that demonstrated a similar relationship between cognitive load and cybersickness using EEG measurements.

Our previous work [51, 52] measured postural stability by subtracting baseline Center of Mass measurements from VR measurements, representing one of the few studies recording baseline walking data. The present study extends this work by examining the spatial and temporal balance dynamics within each of the baseline and VR phases independently, rather than as difference metrics. This approach will reveal how baseline stability relates to cybersickness and how balance patterns evolve during VR exposure, providing broader insight into the relationships between natural walking, VR walking, and cybersickness.

3 Overview

The remainder of this paper is structured to systematically build the case for predictive cybersickness assessment in mobile VR. Section 4 details our data processing pipeline, Section 5 presents our analytical framework, Section 6 reports our statistical findings, Section 7 describes our machine learning model development, Section 8 explains the model results, and Section 9 synthesizes these findings within the broader context of Postural Instability Theory and examines implications for mobile VR design and screening protocols.

4 Data Collection, Preparation and Processing

This study used motion capture data from our previous within-subjects VR experiment on translational gain effects in locomotion and cybersickness [51, 52]. The dataset comprised 3D positional coordinates of all motion-capture markers, participant self-reported sickness ratings (1–10 scale), and associated experimental metadata.

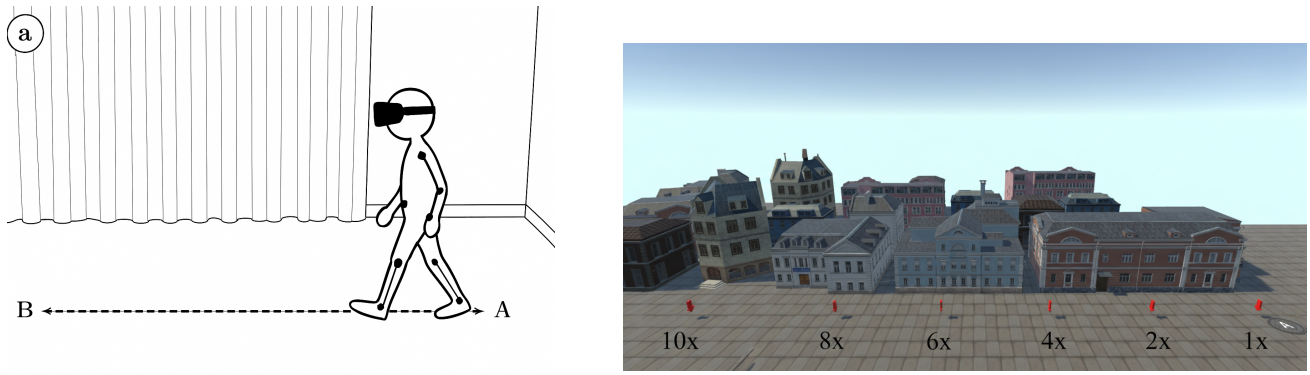

(a) Physical walking area.

(b) Virtual walking area with gain levels.

Fig. 2: Side by side view of the physical and the virtual walking spaces.

4.1 Data Recording and Experiment Design

Experiment Structure

The study employed a progressive exposure methodology to investigate VR sickness through controlled manipulation of translational gain across six escalating levels (1×, 2×, 4×, 6×, 8×, 10×). Each participant completed 30 trials organized into six blocks of five trials each, with translational gain systematically intensified from natural 1:1 mapping to 10× amplification. The experimental protocol deliberately avoided randomization, instead using a fixed ascending sequence to prevent carry-over effects from early exposure to high-gain levels [21].

During each trial, participants started from a virtual utility hole marked as A in both Figures 2a and 2b. Users walked towards the objective marked as B in both Figures 2a and 2b. Then, they turned and walked back towards the original starting point marked as A. This procedure constituted one trial. The objective was marked by red arrows in the virtual environment (see Figure 2b, with the virtual distance traveled expanding proportionally to the gain level while physical walking distance remained constant.

This implementation applied omnidirectional motion magnification rather than forward-only amplification, ensuring continuous postural instability throughout the experience. Post-experiment, participants were categorized into two groups: those with VR sickness (VRS) and those without VR sickness (NoVRS) based on symptom severity.

Experiment Flow

Figure 3 shows the complete experiment procedure. The session began with a *pre-experiment questionnaire (PEQ)* assessing participants' familiarity with 3D and VR technologies and their self-reported susceptibility to motion sickness.

After the PEQ, the researcher fitted the participant with the motion capture suit and verified that full-body motion within the experiment area was successfully captured and displayed. Once the motion capture system was ready, participants performed baseline walking trials without the VR headset, walking from position A to position B, and back to position A as shown in Figure 2a.

The researcher then fitted the VR headset and adjusted the interpupillary distance. The main experiment consisted of six blocks, each with five trials, at increasing TG levels from $1x$ to $10x$. In each trial, participants walked toward a red arrow and back to the utility hole (Figure 2b) in the virtual city. Upon reaching the utility hole, a virtual message confirmed the completion of the trial. It prompted participants to respond to the researchers' between-trial questionnaire.

Each trial lasted an average of 16 seconds, and the total experimental time, including motion capture setup and calibration, was 25 minutes.

Participant Information

The dataset contains information from 21 healthy adults (17 males, four females). The mean age was 25.73, with a standard deviation of 3.594. All participants had a normal or corrected-to-normal vision. Among all participants, 13 had prior experience with three-dimensional computer games, 9 with VR, and 15 had previously experienced motion sickness of varying severity. The study was approved by the Human-Research Ethics Committee of the University of Technology, Sydney. All participants provided written informed consent prior to participation.

Questionnaire Data

The dataset contains responses to two questionnaires. A *Between-Trial Questionnaire* that asks participants to rate six symptoms (dizziness, discomfort, nausea, fatigue, headache, and eyestrain) on a scale from 1 to 10 at the end of each trial. And a *Post-Experiment Simulator Sickness Questionnaire*, used to categorize participants into *VRS* (the group with problematic levels of cybersickness) or *NoVRS* (the group with little or no symptoms).

We based our division on the SSQ severity classification proposed by Kennedy et al. [16] and applied to virtual environments by Stanney et al. [45] which indicates that scores between 15 to 20 represent symptoms of concern. Previous research by Arcioni et al. [1] reported that participants who did not experience cybersickness (as determined via a binary yes/no classification) in an HMD-based VR study had a mean SSQ total score of M = 16.64 (SD = 12.36). Given the established 15-20 symptom concern range and Arcioni's non-sick group averaging 16.64, we selected 18 as a conservative cutoff.

4.2 Data Processing and Cleaning

Building on this dataset, our study begins with data processing and cleaning to derive features relevant for subsequent analysis. All our analyses were performed in Python.

The first data processing step involved computing the CoM for each frame. We followed the process described by Lafond et al. [19] to compute the CoM from the marker locations. We also extracted head movement data from a marker worn on each participant's head.

The raw kinematic recordings contained segments unrelated to forward walking (e.g., waiting, turning, answering questionnaires) and high-frequency noise from the motion capture system. To remove noise generated at these stages, two preprocessing-aware filters were developed to detect the onset of purposeful walking, and a robust smoother was designed to suppress measurement noise while preserving low-frequency sway.

After all the metrics were calculated for each trial, we divided the trials into experimental blocks. Each experimental block consisted of 5 trials, representing each level of gain in the experiment. We grouped the data into experimental groups to observe the evolution of sickness levels and instability metrics over the course of the experiment.

Path Filtering

Because the turns during the experiment generated substantial noise in the walking trials, we developed an algorithm that detects when the user is turning and removes that data from the analysis. The filtering logic is summarized in Table 5 in the Appendix A. This filter avoids ad-hoc time

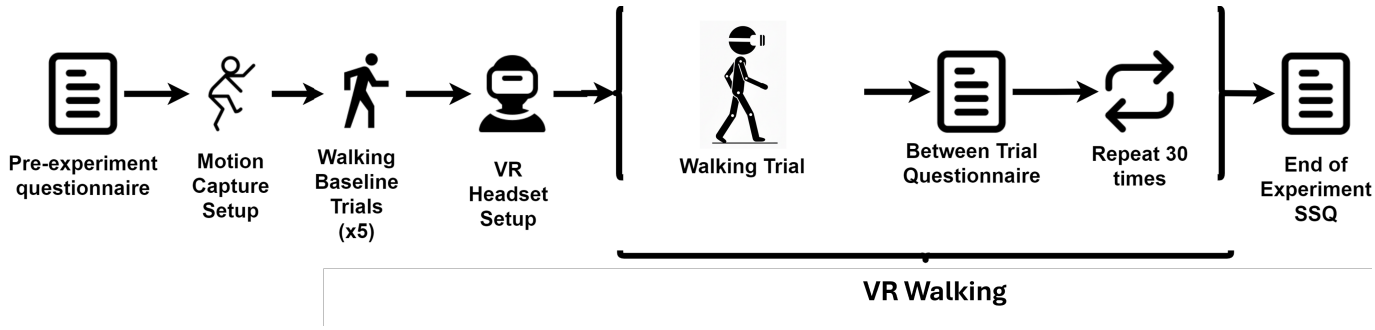

Fig. 3: Flow of the experiment session.

thresholds; trials are aligned at the onset of forward motion, ensuring subsequent kinematic measures are comparable across participants.

The result from this procedure was that each trial was divided into halves. The first half consisted of forward walking (walking from point A to point B). The second half involved walking back (from point B to point A).

Path Smoothing

After removing data from the turns, we attenuated sensor noise by smoothing the signal while retaining the natural sway dynamics of the CoM and head movement. We compared existing filters such as the *1-Euro filter* [3] and FFT [9]. However, FFT introduces phase distortion, and the 1-Euro filter may cause staircase artifacts. We therefore designed a one-pass smoother summarized in Table 6 from Appendix A.

The first half of the algorithm removes outliers by flagging frames where speed exceeds the threshold k_s (to catch sudden position jumps) and where acceleration exceeds the threshold k_a (to catch jittery motion), both set to 3 standard deviations. The second half applies signal smoothing by combining median filtering (to suppress spikes) with Savitzky–Golay filtering, which preserves features like peak height and width while reducing noise [39] and maintaining temporal alignment. The resulting trajectory $\widetilde{\mathscr{P}}$ retains biologically meaningful sway, which is essential for later analyses.

After this process, we removed two participants from our analysis due to excessive motion capture noise.

5 Analysis Methods

After the CoM calculation and data cleaning were completed, we began calculating various spatial and temporal metrics for our analysis.

5.1 Instability Metrics

First, we calculated the multiple instability metrics used in our analysis. These metrics are the Magnitude Difference, Forward Difference, Vertical Difference, and the Lateral Difference.

Analysis began by extracting the first and last data points of each trial as start and end positions. A straight-line trajectory was interpolated between these points to match the temporal resolution of the original CoM data. This reference trajectory served as a baseline for calculating movement deviations. The same interpolation procedure was applied to head movement data to quantify head instability during trials.

These two arrays are compared later to calculate the instability metrics. Each value was paired with another value along what we called the *expected path* line. Figure 4 shows an example of how the 3D data plots looked in relation to the expected path line.

The primary metric calculated was the magnitude difference between corresponding 3D coordinate pairs. For each pairing of 3D points, the magnitude of the difference vector was computed between the biomechanical marker (CoM or head coordinate) and its corresponding point on the *expected path* line.

Calculations were performed for the forward and lateral displacement components, using the x and z coordinates of the biomechanical

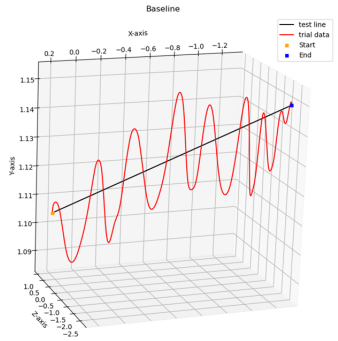

Fig. 4: Example of expected path plot.

marker and the corresponding expected path point. Vertical displacement calculations were performed by subtracting the y-values of the corresponding coordinate pairs.

This code implements a vector decomposition that decomposes spatial displacement into directional components. The first step is to compute the displacement vector by subtracting one point from another. This displacement vector represents the spatial deviation in 2D space. The second operation projects this displacement vector onto a reference direction. This projection captures how much of the total displacement occurs along the forward or backward movement relative to an expected path.

The final calculation determines the perpendicular component via the cross product of the original displacement vector and its projection. This cross product yields the component of the displacement orthogonal to the reference direction. Together, these two components, the parallel projection and the perpendicular cross product, provide a complete decomposition of the spatial deviation into directional components that can be analyzed separately for forward/backward and lateral movements.

5.2 Temporal Analysis

To calculate the temporal characteristics of the biomechanical markers, we employed a Detrended Fluctuation Analysis (DFA) [13]. Center-of-mass data derived from human walking exhibit high variability, which other methods may interpret as noise. DFA overcomes this by detrending locally at multiple scales, isolating the genuine long-range correlations from slow drifts or trends [5]. This method has been extensively used in studies that try to understand temporal characteristics of human biomechanics [5, 10, 14, 23, 26] and to study the relationship between temporal characteristics of human movement and their reported levels of cybersickness [1, 18, 27, 31, 47].

The temporal structure of the data was quantified using the scaling exponent α per axis, which reflects the predictability and persistence of fluctuations across time scales. Specifically, $\alpha \approx 0.5$ indicates white noise, i.e., a completely random signal [11, 33, 35]. Values between 0.5 and 1.0 suggest predictable yet flexible dynamics, where current

patterns influence future ones [8, 11, 26, 33, 35]. An $\alpha \approx 1$ has often been associated with healthy movement [35], though others caution that further evidence is needed before treating it as a definitive marker [11]. Values between 1 and 1.5 indicate stronger correlations and tighter patterns [11, 35], while $\alpha \geq 1.5$ reflects excessive rigidity that may hinder adaptive motor control during walking [35].

5.3 Statistical Analysis

The same procedure is applied to the Center of Mass and Head data for all metrics in both the spatial and temporal analyses. The first step consisted of evaluating data normality by generating and visually inspecting quantile-quantile (QQ) plots, in which deviations from the diagonal reference line indicated departures from normality. All data from the questionnaires were assumed not to follow a normal distribution.

If the data were normally distributed, an independent-samples t-test was conducted using the *scipy* Python module to compare the sick and non-sick groups. Afterwards, effect sizes were quantified using Cohen's d (with Hedges' g as a small-sample correction) along with corresponding confidence intervals.

If the data did not follow a normal distribution, a Kruskal-Wallis H test was conducted using the *scipy* Python module. Afterwards, an epsilon squared (ε^2) was reported as a measure of effect size with 95% confidence intervals. Following Cohen [6], we interpret $\varepsilon^2 \geq 0.26$ as a large effect.

6 Analysis Result

Overall, we discarded data from 5 of 21 participants, leaving 16 for our analysis. Four of those participants had previously reported experiencing a malfunction during data collection. Furthermore, during our analysis, we removed an additional participant because the data were incompatible with our data cleaning procedures and consistently lost full experiment trials after processing them through our Path Filtering and Path Smoothing.

Post-Experiment Questionnaire Results

Based on the questionnaire results, 8 participants were classified in the *VRS* group, and 8 were in the *NoVRS* group. Each group had 2 female participants. From the *VRS* group, 3 participants terminated the experiment before block 6 due to severe VR sickness symptoms at blocks 3, 4, and 5, respectively.

The *VRS* group had a Total Score of $\mu = 39.4850, \sigma = 17.378$, Nausea score of $\mu = 47.7, \sigma = 19.7497$, Occulomotor score of $\mu = 41.69, \sigma = 35.0886$ and Disorientation score of $\mu = 107.88, \sigma = 44.488$. The *NoVRS* group consisted of 8 participants with a TS score of 18 or lower. The *NoVRS* group had Total Score of $\mu = 6.0225, \sigma = 5.3411$, Nausea score of $\mu = 14.31, \sigma = 11.4025$, Occulomotor of $\mu = 9.475, \sigma = 13.2843$ and Disorientation score of $\mu = 12.18, \sigma = 15.6738$.

Between-Trial Questionnaire Results

Most participants experienced symptoms of cybersickness during the experiment, with all groups suffering from dizziness. Fatigue, Headache, and Eyestrain symptoms were rarely reported by participants in both groups. These symptoms averaged below 2 out of 10 throughout the experiment for the *VRS* group and averaged around 1 for the *NoVRS* group. For that reason, those symptoms were discarded from the analysis, and we focused on the Discomfort, Nausea, and Dizziness scores.

Statistical analysis revealed significant differences in discomfort scores between groups. The *NoVRS* group had significantly lower discomfort scores than the *VRS* group in experimental blocks 3 and 4. Table 1 shows a summary of this analysis. A summary of the rest of the symptoms analyzed is available in the supplementary material.

Measure	Block	Statistic, p-val	μ	σ
Discomfort	3	$H(13) = 4.93$, 0.026	*VRS* 3.77 *NoVRS* 1.58	2.14 0.98
Discomfort	4	$H(13) = 4.67$, 0.031	*VRS* 4.40 *NoVRS* 1.75	2.70 1.30

Table 1: Questionnaire responses with significant differences. The third column shows the statistic and p-value. The remaining two columns show the mean and the standard deviation.

Block Analysis

At each experimental block, we tested for a statistical difference between the *VRS* and the *NoVRS* groups. We tested to determine which blocks showed a statistical difference between the two groups. We also tested which experimental blocks are different from the Baseline No-VR condition.

Tables 2 and 3 show results for Center of Mass and Head Movement, respectively. In these tables, we have highlighted with colored squares the experiment blocks in which we found a significant difference between the two groups, and within each group, the comparison to baseline. **Dark blue** showcases blocks where a statistically significant difference was found **and** where a strong effect size ($d \geq 0.8$ for parametric tests, $\varepsilon^2 \geq 0.26$ for non-parametric tests) with confidence intervals excluding zero was observed. **Dark yellow** squares indicate blocks where there was a statistically significant difference ($p < 0.05$), but the confidence intervals crossed zero, indicating insufficient evidence that the observed effect is representative of the population. Across all comparisons in our dataset, statistically significant results fell cleanly into these two categories, with no intermediate cases observed in which significance was accompanied by weak effect sizes and non-zero-crossing confidence intervals.

7 Prediction Model

The observed differences in vertical movement across both spatial and temporal metrics for center of mass and head movement motivated the development of a classification model. This model is intended to quantify the relative importance of vertical displacement compared to other kinematic features in cybersickness prediction. The model incorporated all four kinematic directions (vertical, lateral, forward, and magnitude) for both spatial and temporal feature types. This comprehensive approach enabled us to identify which movement directions and feature types yielded the strongest predictive signals. We performed three tests: combined, spatial-only, and temporal-only. We conducted this test to directly compare the performance of spatial versus temporal features, providing insights into whether static movement characteristics or dynamic temporal patterns better capture cybersickness susceptibility in mobile VR environments.

We trained a binary classifier to predict cybersickness (sick vs. non-sick) from window-level kinematic descriptors derived from head and CoM trajectories. Predictions were aggregated across windows, and performance was reported at the *participant level*, aligning evaluation with individual susceptibility.

Feature Engineering

For each fixed-duration window and each anatomical axis (magnitude, lateral, vertical, forward), we extracted a diverse set of *spatial descriptors*, including measures of central tendency (mean, median), variability (standard deviation, interquartile range, median absolute deviation, root-mean-square), extrema (minimum, maximum, peak-to-peak range), and dynamic characteristics (zero-crossing rate, length-normalized peak count). To capture *temporal dynamics*, we further incorporated DFA features, using the mean α value per window. All descriptors were aligned by *(Participant, Source, Window Index)* to form the design matrix.

Preprocessing

Time-series gaps were handled via linear interpolation during data cleaning (Section 4.2), with any residual missing values imputed feature-wise using the mean. Features were standardized to zero mean and unit variance. To reduce dimensionality, we applied univariate feature selection (`SelectKBest` with ANOVA f-score), retaining at

CoM Measurement	Comparison	Spatial							Temporal (α)						
		BL	1	2	3	4	5	6	BL	1	2	3	4	5	6
Magnitude	VRS vs NoVRS														
	VRS vs BL														
	NoVRS vs BL														
Lateral	VRS vs NoVRS														
	VRS vs BL														
	NoVRS vs BL														
Vertical	VRS vs NoVRS														
	VRS vs BL														
	NoVRS vs BL														
Forward	VRS vs NoVRS														
	VRS vs BL														
	NoVRS vs BL														

Table 2: Summary of Spatial and temporal results for the Center of Mass. Blue indicates strong effects (Cohen's $d \geq 0.8$ for parametric, $\varepsilon^2 \geq 0.26$ for non-parametric) with CI that do not cross 0. Orange indicates statistically significant with no effect, and gray indicates no difference. BL = Baseline (No-VR walking).

HM Measurement	Comparison	Spatial							Temporal (α)						
		BL	1	2	3	4	5	6	BL	1	2	3	4	5	6
Magnitude	VRS vs NoVRS														
	VRS vs BL														
	NoVRS vs BL														
Lateral	VRS vs NoVRS														
	VRS vs BL														
	NoVRS vs BL														
Vertical	VRS vs NoVRS														
	VRS vs BL														
	NoVRS vs BL														
Forward	VRS vs NoVRS														
	VRS vs BL														
	NoVRS vs BL														

Table 3: Summary of spatial and temporal results for the Head Movement (HM). Blue indicates strong effects (Cohen's $d \geq 0.8$ for parametric, $\varepsilon^2 \geq 0.26$ for non-parametric) with CI that do not cross 0. Orange indicates statistically significant with no effect, and gray indicates no difference. BL = Baseline (No-VR walking).

least $k \geq 40$ descriptors to preserve diversity. DFA-only models did not require feature selection.

Classifier and Cross-Validation

We trained a ℓ_2-regularized logistic regression model with class balancing to address class imbalance between sick and non-sick cases. To implement this balancing, we applied inverse-frequency class weighting within the ℓ_2-regularized logistic regression model. Let N denote the total number of samples and N_c the number of samples belonging to class c. The weight assigned to each class was defined as

$$w_c = \frac{N}{2N_c},$$

giving the minority (VRS group) class proportionally higher influence in the loss function. This adjustment ensures that both classes contribute comparably during optimization and prevents the model from being biased toward the majority class. This weighting scheme corresponds to the standard "balanced" strategy commonly used in statistical learning frameworks. This correction was particularly relevant for VR trial models, where the VRS group completed fewer trials due to symptom severity; baseline models used balanced data Logistic regression was selected because it yields interpretable coefficients, converges reliably with small datasets, and enables us to identify which gait features are most strongly associated with cybersickness.

To avoid *identity leakage*, we employed GroupKFold cross-validation, assigning all windows from a given participant exclusively to either the training or test set. Depending on cohort size, we used $K = 2$ or 3 folds to ensure multiple participants appeared in each test split. Within each fold, contributions were normalized so that every participant had equal influence, preventing bias from individuals with more recorded windows.

This approach prioritizes interpretability and participant-level validity, allowing us to directly connect model outcomes to Postural Instability Theory by showing how specific aspects of gait stability predict susceptibility to cybersickness in mobile VR.

Pooling from Windows to Participants

Let $\hat{p}_{k,i}$ be the predicted probability for window i of participant k and n_k the number of test windows for k. We report two pooling rules:

$$\bar{p}_k^{\text{mean}} = \frac{1}{n_k}\sum_{i=1}^{n_k}\hat{p}_{k,i}, \qquad \ell_{k,i} = \log\frac{\hat{p}_{k,i}}{1-\hat{p}_{k,i}},$$

$$\bar{\ell}_k = \frac{1}{\tau}\log\Big(\frac{1}{n_k}\sum_{i=1}^{n_k} e^{\tau\ell_{k,i}}\Big), \quad \bar{p}_k^{\text{LSE}} = \sigma(\bar{\ell}_k),$$

where $\sigma(\cdot)$ is the logistic function. The LogSumExp pooling temperature was fixed to τ=1.5, which emphasizes confident windows while avoiding over-reliance on single outliers; this value was chosen after preliminary trials indicated it provided stable performance across participants.

Evaluation and Uncertainty Quantification

For each fold, area under the ROC curve (AUC) and accuracy (ACC; threshold 0.5) were computed on participant-level pooled predictions; fold means and standard deviations summarize cross-validated performance. In addition, one out-of-fold (OOF) probability per participant was obtained, and a 95% CI for the OOF AUC was estimated by nonparametric bootstrap resampling over participants (B=2000), providing a measure of robustness to sample variability.

Model Interpretation with SHAP

Post hoc explanations used a linear SHAP explainer on the preprocessed feature space. Participant-level attributions were averaged to estimate overall importance, and features were grouped by anatomical axis to highlight biomechanical structure. In combined models, contributions were also separated by family (spatial statistics vs. DFA), enabling direct comparison of spatial and temporal predictors of cybersickness.

Analytical Conditions

Three pre-specified configurations are analyzed in parallel: (i) **Spatial-only** (spatial descriptors of head/CoM), (ii) **α-only** (DFA exponents per axis), and (iii) **Spatial+α** (concatenated features). For each configuration, we trained and evaluated on (a) all sources combined, and separately on (b) Head-only and (c) CoM-only subsets, enabling direct comparison of predictive anatomy across sources.

8 Prediction Model Result

Multiple feature configurations are evaluated (spatial descriptors, temporal descriptors, and combined features) derived from head motion, center of mass (CoM), and their combination.

To aggregate temporal predictions, we considered two pooling strategies: (i) **mean pooling**, which computes the arithmetic average across frames to capture overall trends, and (ii) **log-sum-exp (LSE) pooling**, which acts as a soft maximum and emphasizes short, highly discriminative segments.

CoM spatial features from baseline walking achieved AUC = 0.761 (95% CI [0.476, 0.983]) using logistic regression with participant-level cross-validation. SHAP feature importance analysis showed vertical movement contributed 44.4% of predictive power, lateral movement 23.0%, magnitude 22.4%, and anterior-posterior movement 10.2%.

Temporal features alone yielded an AUC of 0.561 (95% CI [0.250, 0.883]) for CoM analysis. Head movement spatial features achieved AUC = 0.404 (95% CI [0.102, 0.714]), while head movement temporal features achieved AUC = 0.512 (95% CI [0.206, 0.818]).

Combined spatial and temporal features produced AUC = 0.667 (95% CI [0.365, 0.921]) for center of mass analysis and AUC = 0.686 (95% CI [0.391, 0.927]) for all features combined. Bootstrap confidence intervals were computed using B=2000 resamples to assess statistical robustness across all analyses. Cross-validation performance showed a mean AUC of 0.648 $\pm$ 0.386 (standard deviation across folds) for CoM spatial features, with accuracy = 0.644 $\pm$ 0.220. In addition to accuracy and AUC, average precision (AP) and F1-score were reported to complement threshold-independent evaluation with class-sensitive performance measures. Across both baseline and experimental conditions, models using spatial features or combined spatial and temporal features generally achieved higher AP values (up to $\approx$ 0.8) than temporal-feature–only models, consistent with the trends observed for AUC. In contrast, F1-scores remained moderate (typically $\approx$ 0.45–0.65) and exhibited larger variability across cross-validation folds.

For full predicted performance metrics, see Appendix C.

Feature Contributions

Axis-level SHAP analysis was conducted to quantify feature importance across movement directions for the center of mass spatial model using baseline walking data. The analysis computed the relative contributions of each movement axis to the overall predictive performance.

Axis	Importance
Vertical	0.444
Lateral	0.230
Magnitude	0.224
Forward	0.102

Table 4: Axis-level SHAP importances (Center of Mass spatial features, Baseline condition)

The vertical axis contributed 44.4% of the total feature importance, followed by lateral (23.0%), magnitude (22.4%), and forward movement (10.2%). Complete SHAP importance values for all experimental conditions and feature combinations are provided in Appendix C.

9 Discussion

9.1 Before VR Exposure

Building on Postural Instability Theory (PIT), we investigated whether naturally unstable participants would also suffer from cybersickness in mobile VR contexts [1, 37, 49]. To this end, we analyzed both spatial and temporal dynamics of center of mass (CoM) movement during baseline walking, hypothesizing that pre-VR differences would distinguish future cybersickness-susceptible individuals. We observed significant spatial differences in CoM kinematics between groups during No-VR walking, particularly in forward and vertical movements, where the cybersickness-susceptible group showed greater displacement. Surprisingly, we found no temporal differences in the same scenario, in contrast to previous non-locomotive postural studies [7, 27, 47].

Machine learning analysis using SHAP (SHapley Additive exPlanations) revealed that vertical movement of the center of mass was by far the strongest predictor of cybersickness susceptibility, accounting for 44.4% of the predictive power in our logistic regression model. This was followed by lateral movement (23.0%) and magnitude (22.4%), while forward movement contributed only 10.2%. These findings demonstrate that pre-VR walking assessments can effectively identify individuals susceptible to cybersickness, with vertical movement serving as the primary feature.

The work by Arcioni et al. [1] reported findings similar to ours, with differences in forward movement among participants but none in lateral movement. Vertical movements of the CoM during gait cycles reflect differences in gait strategies, with increases in vertical movement linked to increases in walking speed [48]. The dominance of vertical movement as a predictor (44.4% vs 10.2% for forward movement) suggests that mechanisms underlying cybersickness in locomotive contexts are fundamentally different from non-locomotive contexts, where anterior-posterior sway typically dominates.

Importantly, when comparing body segments, center of mass metrics outperformed head movement for prediction, with CoM vertical movement (44.4%) substantially outperforming the best head predictor (lateral head movement at 36.2%). This suggests that cybersickness susceptibility reflects whole-body postural control differences rather than head-specific sensory processing deficits. These results provide an important constraint on sensory conflict theory (Kim et al. [17]), which emphasizes visual-vestibular mismatches. Since vestibular organs signal head motion, a purely sensory conflict account would predict that head movement is the stronger predictor. Our finding that CoM displacement is more predictive suggests that postural instability theory captures mechanisms beyond visual-vestibular conflict alone.

The prominence of vertical movement reflects fundamental biomechanics of the gait cycle, where increases in vertical displacement typically correspond to decreases in lateral movement [29]. Previous research demonstrates that increased walking speed in healthy individuals

can induce temporary postural instability, but the body's sensorimotor system appears to adapt and recover stability through repeated exposure [38, 50]. More work is needed to determine whether this pre-VR walking behavior is due to the participants' natural instability or to preferred walking mechanics that influence the likelihood of cybersickness in walking VR environments.

9.2 Influence of VR and Translational Gain

VR introduction universally modifies the walking mechanics of users [2, 12]. However, our analyses revealed that baseline spatial differences persisted between the groups after VR was introduced. Furthermore, the introduction of VR generated temporal differences in vertical CoM movement, which emerged for the first time, indicating VR's challenge to movement coordination.

The introduction of translational gain (Block 2) triggered divergent adaptation strategies. Both groups exhibited more rigid movement patterns (temporal values <1.5) [35], but the cybersickness group showed significantly greater rigidity. This suggests a "safety-first" strategy that prioritizes control over flexibility, paradoxically increasing susceptibility to cybersickness, as reported previously [52].

9.3 Symptom Manifestation

Blocks 3-4 marked the critical transition from biomechanical differences to conscious symptom recognition, as questionnaire responses first diverged between groups at the discomfort metric. We observe significant differences in magnitude both spatially and temporally, as well as in vertical and lateral directions (and in the next block, in forward movement). Spatial and temporal head-movement changes begin to appear at this stage, especially laterally.

The consistent differences in postural instability metrics, particularly vertical movement patterns, observed before symptom manifestation support the core tenets of Postural Instability Theory (PIT), which posits that instability precedes subjective cybersickness symptoms [36]. Similar pre-symptomatic changes have been documented in walking environments using physiological measures [52]. These findings demonstrate that objective biomechanical and physiological differences between participant groups emerge before users report subjective symptom changes, suggesting the potential for early detection approaches.

Not only did we observe a significant difference between the two groups across almost all spatial and temporal metrics, but we also observed a general decline in vertical movement during this symptomatic phase. This is consistent with previous research on walking in VR environments, which reports that participants typically take longer to complete trials during symptomatic phases [51, 52]. However, despite an overall speed reduction, the *VRS* group maintained relatively higher walking speeds than the *NoVRS* group, as evidenced by their persistently greater vertical movement [48].

This pattern reinforces vertical movement as a key predictor of cybersickness: even when both groups slow down in response to VR challenges, the relative difference in vertical displacement persists, suggesting that this metric captures fundamental differences in gait strategy rather than simply speed variations. The cybersickness-susceptible group's inability to reduce their vertical movement to the same extent as controls may reflect less flexible postural adaptation strategies.

9.4 Temporal Dynamics Analysis

After failing to identify any temporal differences during the NoVR session, the main experiment session revealed temporal differences in both groups. Throughout the experiment, the temporal dynamics of the vertical movement of the *NoVRS* group showed mean DFA alpha values between 0.9 and 1, which is considered patterned yet flexible and is observed in healthy walking dynamics [8, 11, 26, 33, 35]. This demonstrates self-similarity more consistent with pink-noise characteristics ($\alpha \approx 1.0$) than with white-noise characteristics ($\alpha \approx 0.5$), indicating structure rather than random movement patterns. These alpha values demonstrate not only the flexibility of their walking patterns but also their ability to maintain and manage postural challenges throughout the VR session [34].

In contrast, the cybersickness-susceptible group consistently exhibited vertical alpha values above 1.0, suggesting self-similarity more characteristic of Brownian noise ($\alpha > 1.0$). This indicates rigid, overconstrained movement patterns. This finding aligns with previousnon-locomotive cybersickness research that reported natural rigidity in participants who later developed motion sickness [43, 47]. Our results demonstrate that movement rigidity in the vertical axis consistently serves as a key feature of cybersickness susceptibility across this dataset.

This temporal rigidity likely reflects increased neural control demands, consistent with previous mobile VR research reporting elevated cognitive load and gait adaptation in cybersickness-susceptible participants [52]. The rigid walking patterns we observed may both result from and contribute to this increased processing burden. Supporting this interpretation, Ortega and Farley [30] demonstrated that managing vertical movement during locomotion increases metabolic cost, suggesting that the rigid postural control strategies adopted by cybersickness-susceptible individuals impose additional physiological and cognitive demands that may exacerbate their symptoms.

9.5 Spatial vs Temporal Dynamics

Spatial features demonstrated better predictive performance compared to temporal features during VR exposure. Center of mass spatial analysis achieved robust prediction (AUC = 0.761, 95% CI [0.476, 0.983]), while temporal features yielded substantially lower performance (AUC = 0.561). This difference indicates that spatial movement patterns carry the primary predictive information for susceptibility to cybersickness during virtual environment exposure.

Our analysis reveals how the temporal dynamics of VR walking facilitate an understanding of the differences in movement and adaptation between the two groups. Spatial metrics reveal their postural control abilities and demonstrate that they have the most predictive power for cybersickness susceptibility.

9.6 Vertical Movement

Vertical movement emerges as the predictor that offers the greatest diagnostic leverage in our dataset, accounting for 44.4% of the spatial predictive importance during VR. This exceeds lateral movement (23.0%), magnitude (22.4%), and anterior-posterior movement (10.2%) in our experimental conditions. The difference between vertical (44.4%) and anterior-posterior (10.2%) importance suggests that cybersickness susceptibility may involve direction-specific rather than general postural differences, though this requires validation across different VR environments. Our findings indicate that vertical center of mass displacement shows promise as a marker in mobile VR contexts.

The prominence of vertical movement in our mobile paradigm suggests that walking-based cybersickness assessment may emphasize different movement patterns than non-locomotive studies. This raises the possibility that mobile cybersickness may represent a combination of postural instability and gait control mechanisms rather than postural instability alone.

10 Future Work

Our No-VR results show promise in identifying participants susceptible to cybersickness in mobile environments. Future work should test whether these findings are replicable in other types of walking virtual environments. Future work should also develop a calibration session for walking in VR.

The metrics used during our analysis should be validated in different VR walking environments. Changes such as free-walking rather than straight walking, the distance walked, and the duration walked should be tested to determine whether these metrics differ in their ability to measure cybersickness.

More research is needed on understanding how locomotion strategies affect the level of cybersickness experienced. These changes can inform our future approaches to predicting and intervening in cybersickness across diverse environments.

Building on our kinematic findings and from Weech et al.'s [53] demonstration that kinematics outperformed vestibular and vection

measures, future work should compare kinematic versus physiological prediction and assess potential benefits of multimodal integration.

Previous studies have demonstrated that both physiological and biomechanical changes precede the onset of subjective cybersickness symptoms [41, 52]. By combining these complementary measurement approaches with appropriate machine learning methods, it may be possible to develop predictive models that detect the onset of cybersickness before users experience sufficient discomfort to terminate their VR sessions. Such early-detection systems could enable proactive interventions to mitigate symptoms and improve the VR user experience.

11 Limitations

One of the main limitations of this work is the sample size for the experiments. We need a larger sample of participants to yield more significant, more generalizable results. While we calculated the effect size to assess the strength of our results, having more participants in the experiment will yield stronger results.

The sample size, which yielded wide confidence intervals in our Machine Learning Classification, also influenced our Machine Learning analysis. The automatic feature selection, and the focus on binary classification, should all be expanded in future studies.

Another limitation is using a single numerical cutoff to distinguish sick from non-sick groups. Future work should complement the post-experiment SSQ with forced-choice questions to improve participant classification.

12 Conclusion

This study demonstrates that susceptibility to cybersickness can be predicted prior to VR exposure using baseline walking assessment. Vertical center of mass displacement emerged as the primary predictive feature, substantially outperforming other movement directions and establishing a foundation for proactive cybersickness screening.

Our analysis revealed a timeline of events as cybersickness develops through different experimental stages. Spatial differences are detectable before VR exposure, temporal changes emerge during VR introduction, and subjective symptoms appear last through the middle of the experiment. This progression suggests multiple opportunities for intervention throughout the development of cybersickness.

These findings extend postural instability theory to mobile contexts, demonstrating that cybersickness susceptibility reflects intrinsic movement signatures related to gait control mechanisms rather than solely traditional postural sway. Center of mass assessment proved superior to head movement analysis, supporting whole-body evaluation approaches.

This research enables the development of practical screening protocols specifically for mobile VR applications, moving from reactive symptom management to predictive risk assessment in walking-based virtual environments. The ability to identify susceptible individuals before mobile VR exposure supports personalized locomotion experiences and could prevent negative first encounters with walking-based virtual reality applications.

Acknowledgments

The authors thank the anonymous reviewers for their insightful comments, which helped improve the quality and presentation of this paper.

References

[1] B. Arcioni, S. Palmisano, D. Apthorp, and J. Kim. Postural stability predicts the likelihood of cybersickness in active hmd-based virtual reality. *Displays*, 58:3–11, 7 2019. doi: 10.1016/j.displa.2018.07.001 1, 2, 3, 4, 7

[2] J. B. Bendixen, B. T. Biddinger, J. E. Simon, S. M. Monfort, and D. R. Grooms. Effects of virtual reality immersion on postural stability during a dynamic transition task. *Sports Biomechanics*, 24(4):859–873, 2025. PMID: 36597788. doi: 10.1080/14763141.2022.2162434 8

[3] G. Casiez, N. Roussel, and D. Vogel. 1 € filter: A simple speed-based low-pass filter for noisy input in interactive systems. In *Proceedings of the SIGCHI Conference on Human Factors in Computing Systems*, CHI '12, 4 pages, p. 2527–2530. Association for Computing Machinery, New York, NY, USA, 2012. doi: 10.1145/2207676.2208639 4

[4] S. S. Chance, F. Gaunet, A. C. Beall, and J. M. Loomis. Locomotion mode affects the updating of objects encountered during travel: The contribution of vestibular and proprioceptive inputs to path integration. *Presence: Teleoperators and Virtual Environments*, 7(2):168–178, 04 1998. doi: 10.1162/105474698565659 1

[5] Z. Chen, P. C. Ivanov, K. Hu, and H. E. Stanley. Effect of nonstationarities on detrended fluctuation analysis. *Phys. Rev. E*, 65:041107, 15 pages, Apr 2002. doi: 10.1103/PhysRevE.65.041107 4

[6] J. Cohen. A power primer. *Psychological Bulletin*, 112:155–159, 1992. doi: 10.1037/0033-2909.112.1.155 5

[7] C. Curry, N. Peterson, R. Li, and T. A. Stoffregen. Postural precursors of motion sickness in head-mounted displays: drivers and passengers, women and men. *Ergonomics*, 63:1502–1511, 12 2020. doi: 10.1080/00140139.2020.1808713 1, 2, 7

[8] S. Damouras, M. D. Chang, E. Sejdić, and T. Chau. An empirical examination of detrended fluctuation analysis for gait data. *Gait & Posture*, 31:336–340, 3 2010. doi: 10.1016/j.gaitpost.2009.12.002 5, 8

[9] M. Frigo and S. Johnson. Fftw: an adaptive software architecture for the fft. In *Proceedings of the 1998 IEEE International Conference on Acoustics, Speech and Signal Processing, ICASSP '98 (Cat. No.98CH36181)*, vol. 3, pp. 1381–1384 vol.3, 1998. doi: 10.1109/ICASSP.1998.681704 4

[10] J. Gao, J. Hu, W.-W. Tung, Y. Cao, N. Sarshar, and V. P. Roychowdhury. Assessment of long-range correlation in time series: How to avoid pitfalls. *Phys. Rev. E*, 73:016117, 10 pages, Jan 2006. doi: 10.1103/PhysRevE.73.016117 4

[11] R. Hardstone, S.-S. Poil, G. Schiavone, R. Jansen, V. V. Nikulin, H. D. Mansvelder, and K. Linkenkaer-Hansen. Detrended fluctuation analysis: A scale-free view on neuronal oscillations. *Frontiers in Physiology*, 3:23105, 11 2012. doi: 10.3389/fphys.2012.00450 4, 5, 8

[12] J. H. Hollman, R. H. Brey, T. J. Bang, and K. R. Kaufman. Does walking in a virtual environment induce unstable gait?: An examination of vertical ground reaction forces. *Gait & Posture*, 26(2):289–294, 2007. doi: 10.1016/j.gaitpost.2006.09.075 8

[13] K. Hu, P. C. Ivanov, Z. Chen, P. Carpena, and H. Eugene Stanley. Effect of trends on detrended fluctuation analysis. *Phys. Rev. E*, 64:011114, 19 pages, Jun 2001. doi: 10.1103/PhysRevE.64.011114 4

[14] E. A. Ihlen, N. Skjæret, and B. Vereijken. The influence of center-of-mass movements on the variation in the structure of human postural sway. *Journal of Biomechanics*, 46(3):484–490, 2013. doi: 10.1016/j.jbiomech.2012.10.016 4

[15] O. Janeh, G. Bruder, F. Steinicke, A. Gulberti, and M. Poetter-Nerger. Analyses of gait parameters of younger and older adults during (non-)isometric virtual walking. *IEEE Transactions on Visualization and Computer Graphics*, 24:2663–2674, 10 2018. change the scale / gain of the gait mapping in VR. doi: 10.1109/TVCG.2017.2771520 2

[16] R. S. Kennedy, N. E. Lane, K. S. Berbaum, and M. G. Lilienthal. Simulator sickness questionnaire: An enhanced method for quantifying simulator sickness. *The International Journal of Aviation Psychology*, 3(3):203–220, 1993. doi: 10.1207/s15327108ijap0303_3 3

[17] J. Kim, W. Luu, and S. Palmisano. Multisensory integration and the experience of scene instability, presence and cybersickness in virtual environments. *Computers in Human Behavior*, 113:106484, 12 2020. doi: 10.1016/j.chb.2020.106484 1, 7

[18] F. Koslucher, E. Haaland, and T. A. Stoffregen. Sex differences in visual performance and postural sway precede sex differences in visually induced motion sickness. *Experimental Brain Research*, 234:313–322, 9 2016. doi: 10.1007/S00221-015-4462-Y 1, 4

[19] D. Lafond, M. Duarte, and F. Prince. Comparison of three methods to estimate the center of mass during balance assessment. *Journal of Biomechanics*, 37(9):1421–1426, sep 2004. doi: 10.1016/S0021-9290(03)00251-3 3

[20] J. J. LaViola. A discussion of cybersickness in virtual environments. *SIGCHI Bull.*, 32(1):47–56, 10 pages, Jan. 2000. doi: 10.1145/333329.333344 1

[21] B. D. Lawson and K. M. Stanney. Editorial: Cybersickness in virtual reality and augmented reality. *Frontiers in Virtual Reality*, Volume 2 - 2021, 2021. doi: 10.3389/frvir.2021.759682 3

[22] J. Lee, M. Kim, and J. Kim. A study on immersion and vr sickness in walking interaction for immersive virtual reality applications. *Symmetry*, 9(5), 2017. doi: 10.3390/sym9050078 2

[23] D. Lin, H. Seol, M. A. Nussbaum, and M. L. Madigan. Reliability of

cop-based postural sway measures and age-related differences. *Gait & Posture*, 28(2):337–342, 2008. doi: 10.1016/j.gaitpost.2008.01.005 4

[24] J. Lohman and L. Turchet. Evaluating cybersickness of walking on an omnidirectional treadmill in virtual reality. *IEEE Transactions on Human-Machine Systems*, 52(4):613–623, 2022. doi: 10.1109/THMS.2022.3175407 2

[25] J. Mayor, L. Raya, and A. Sanchez. A comparative study of virtual reality methods of interaction and locomotion based on presence, cybersickness, and usability. *IEEE Transactions on Emerging Topics in Computing*, 9(3):1542–1553, 2021. doi: 10.1109/TETC.2019.2915287 2

[26] J. Munafo, C. Curry, M. G. Wade, and T. A. Stoffregen. The distance of visual targets affects the spatial magnitude and multifractal scaling of standing body sway in younger and older adults. *Experimental Brain Research*, 234:2721–2730, 9 2016. doi: 10.1007/s00221-016-4676-7 4, 5, 8

[27] J. Munafo, M. Diedrick, and T. A. Stoffregen. The virtual reality head-mounted display oculus rift induces motion sickness and is sexist in its effects. *Experimental Brain Research*, 235:889–901, 3 2017. doi: 10.1007/s00221-016-4846-7 1, 2, 4, 7

[28] N. C. Nilsson, S. Serafin, F. Steinicke, and R. Nordahl. Natural walking in virtual reality. *Computers in Entertainment*, 16:1–22, 4 2018. doi: 10.1145/3180658 1, 2

[29] M. Orendurff, A. D. Segal, G. K. Klute, J. S. Berge, E. Rohr, and N. J. Kadel. The effect of walking speed on center of mass displacement. *Journal of rehabilitation research and development*, 41 6A:829–34, 2004. 7

[30] J. D. Ortega and C. T. Farley. Minimizing center of mass vertical movement increases metabolic cost in walking. *Journal of Applied Physiology*, 99(6):2099–2107, 2005. PMID: 16051716. doi: 10.1152/japplphysiol.00103.2005 8

[31] S. Palmisano, R. S. Allison, and J. Kim. Cybersickness in head-mounted displays is caused by differences in the user's virtual and physical head pose. *Frontiers in Virtual Reality*, 1:587698, 11 2020. doi: 10.3389/frvir.2020.587698 1, 4

[32] S. Palmisano, R. S. Allison, J. Teixeira, and J. Kim. Differences in virtual and physical head orientation predict sickness during active head-mounted display-based virtual reality. *Virtual Reality*, 27:1293–1313, 6 2023. doi: 10.1007/s10055-022-00732-5 1

[33] I. Radić, S. Blesić, Z. Aničić, S. Milanović, D. M. Mirkov, and O. M. Knežević. Quantification of changes in balance control with tasks and injury using detrending methods for time series analysis. *Frontiers in Bioengineering and Biotechnology*, 13:1589072, 6 2025. doi: 10.3389/fbioe.2025.1589072 4, 5, 8

[34] R. Rajachandrakumar, J. Mann, A. Schinkel-Ivy, and A. Mansfield. Exploring the relationship between stability and variability of the centre of mass and centre of pressure. *Gait & Posture*, 63:254–259, 2018. doi: 10.1016/j.gaitpost.2018.05.008 8

[35] D. K. Ravi, V. Marmelat, W. R. Taylor, K. M. Newell, N. Stergiou, and N. B. Singh. Assessing the temporal organization of walking variability: A systematic review and consensus guidelines on detrended fluctuation analysis. *Frontiers in Physiology*, 11:534384, 6 2020. doi: 10.3389/fphys.2020.00562 4, 5, 8

[36] G. E. Riccio and T. A. Stoffregen. An ecological theory of motion sickness and postural instability. *Ecological Psychology*, 3:195–240, 9 1991. doi: 10.1207/s15326969eco0303_2 1, 8

[37] D. Risi and S. Palmisano. Effects of postural stability, active control, exposure duration and repeated exposures on hmd induced cybersickness. *Displays*, 60:9–17, 2019. doi: 10.1016/j.displa.2019.08.003 7

[38] P. E. Roos and J. B. Dingwell. Influence of neuromuscular noise and walking speed on fall risk and dynamic stability in a 3d dynamic walking model. *Journal of Biomechanics*, 46:1722–1728, 6 2013. doi: 10.1016/j.jbiomech.2013.03.032 8

[39] A. Savitzky and M. J. E. Golay. Smoothing and differentiation of data by simplified least squares procedures. *Analytical Chemistry*, 36(8):1627–1639, 1964. doi: 10.1021/ac60214a047 4

[40] E. Sayyad, M. Sra, and T. Höllerer. Walking and teleportation in wide-area virtual reality experiences. In *2020 IEEE International Symposium on Mixed and Augmented Reality (ISMAR)*, pp. 608–617, 2020. doi: 10.1109/ISMAR50242.2020.00088 2

[41] J. N. Setu, J. M. Le, R. K. Kundu, B. Giesbrecht, T. Höllerer, K. A. Hoque, K. Desai, and J. Quarles. Mazed and confused: A dataset of cybersickness, working memory, mental load, physical load, and attention during a real walking task in vr. In *2024 IEEE International Symposium on Mixed and Augmented Reality (ISMAR)*, pp. 1048–1057. IEEE, 10 2024. doi: 10.1109/ISMAR62088.2024.00121 1, 2, 9

[42] L. J. Smart, A. Drew, T. Hadidon, M. Teaford, and E. Bachmann. Using nonlinear kinematic parameters as a means of predicting motion sickness in real-time in virtual environments. *Human Factors: The Journal of the Human Factors and Ergonomics Society*, 65:1830–1840, 12 2023. doi: 10.1177/00187208211059623 2

[43] L. J. Smart, E. W. Otten, A. J. Strang, E. M. Littman, and H. E. Cook. Influence of complexity and coupling of optic flow on visually induced motion sickness. *Ecological Psychology*, 26:301–324, 10 2014. doi: 10.1080/10407413.2014.958029 2, 8

[44] K. Stanney and R. Kennedy. *Simulation Sickness*, pp. 117–127. CRC Press, 12 2008. doi: 10.1201/9781420072846.ch6 1

[45] K. M. Stanney, R. S. Kennedy, and J. M. Drexler. Cybersickness is not simulator sickness. *Proceedings of the Human Factors and Ergonomics Society Annual Meeting*, 41:1138–1142, 10 1997. doi: 10.1177/107118139704100292 3

[46] T. A. Stoffregen and L. Smart. Postural instability precedes motion sickness. *Brain Research Bulletin*, 47:437–448, 11 1998. doi: 10.1016/S0361-9230(98)00102-6 1, 2

[47] T. A. Stoffregen, K. Yoshida, S. Villard, L. Scibora, and B. G. Bardy. Stance width influences postural stability and motion sickness. *Ecological Psychology*, 22:169–191, 7 2010. doi: 10.1080/10407413.2010.496645 1, 2, 4, 7, 8

[48] Y. Takeda and T. Watanabe. A feasibility test of evaluation of gait movement by using center of mass estimation with inertial sensors. In J. Henriques, N. Neves, and P. de Carvalho, eds., *XV Mediterranean Conference on Medical and Biological Engineering and Computing – MEDICON 2019*, pp. 718–726. Springer International Publishing, Cham, 2020. 7, 8

[49] J. Teixeira, S. Miellet, and S. Palmisano. Effects of vection type and postural instability on cybersickness. *Virtual Reality*, 28:82, 3 2024. doi: 10.1007/s10055-024-00969-2 7

[50] K. S. Thomas, B. L. VanLunen, and S. Morrison. Changes in postural sway as a function of prolonged walking. *European Journal of Applied Physiology*, 113:497–508, 2 2013. doi: 10.1007/s00421-012-2456-z 8

[51] C. A. Tirado Cortes, H.-T. Chen, and C.-T. Lin. Analysis of vr sickness and gait parameters during non-isometric virtual walking with large translational gain. In *Proceedings of the 17th International Conference on Virtual-Reality Continuum and its Applications in Industry*, pp. 1–10. ACM, 11 2019. doi: 10.1145/3359997.3365694 1, 2, 8

[52] C. A. Tirado Cortes, C.-T. Lin, T.-T. N. Do, and H.-T. Chen. An eeg-based experiment on vr sickness and postural instability while walking in virtual environments. In *2023 IEEE Conference Virtual Reality and 3D User Interfaces (VR)*, pp. 94–104. IEEE, 3 2023. doi: 10.1109/VR55154.2023.00025 1, 2, 8, 9

[53] S. Weech, J. P. Varghese, and M. Barnett-Cowan. Estimating the sensorimotor components of cybersickness. *Journal of Neurophysiology*, 120:2201–2217, 11 2018. doi: 10.1152/jn.00477.2018 2, 8

[54] G. Wilson, M. McGill, M. Jamieson, J. R. Williamson, and S. A. Brewster. Object manipulation in virtual reality under increasing levels of translational gain. In *Proceedings of the 2018 CHI Conference on Human Factors in Computing Systems*, pp. 1–13. ACM, 4 2018. above x2 translational gain -> less accurate and higher sicknessobject selection task, free walking task. doi: 10.1145/3173574.3173673 2

[55] B. Winther, M. L. Krarup, P. N. Andersen, U. Lee, and N. C. Nilsson. Effects of walking together in a co-located virtual reality game. In *2023 IEEE Conference on Virtual Reality and 3D User Interfaces Abstracts and Workshops (VRW)*, pp. 257–262, 2023. doi: 10.1109/VRW58643.2023.00063 2

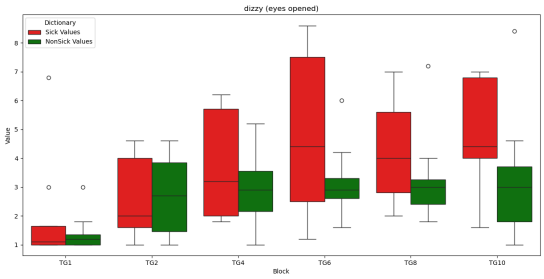

Fig. 5: Overall Dizzy Results

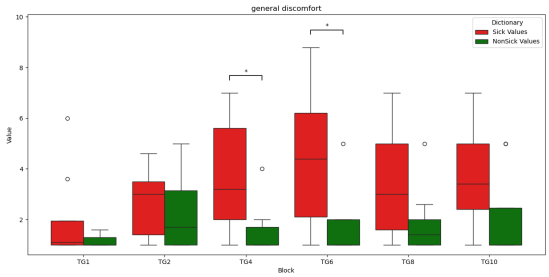

Fig. 6: Overall Discomfort Results

A Algorithm Appendix

Table 5: Workflow of the direction-aware path filter.

Step	Operation and Definitions
1	Define the task axis as $\hat{\mathbf{v}} = (\mathbf{P}_1 - \mathbf{P}_0)/\|\mathbf{P}_1 - \mathbf{P}_0\|$, where $\mathbf{P}_0$ is the start point, $\mathbf{P}_1$ the goal point, and $\hat{\mathbf{v}}$ the unit vector along the task axis.
2	For each displacement $\mathbf{s}_i = \mathbf{x}_i - \mathbf{x}_{i-1}$ with position $\mathbf{x}_i$: (i) check whether the current position is in front of the start, i.e. $(\mathbf{x}_i - \mathbf{P}_0)\cdot\hat{\mathbf{v}} > \varepsilon$, (ii) check whether the step direction is within tolerance, i.e. $\frac{\mathbf{s}_i\cdot\hat{\mathbf{v}}}{\|\mathbf{s}_i\|} \geq \cos(\theta_{\max})$, where ε is a numerical tolerance and $\theta_{\max}$ the angular threshold.
3	Identify the first index $i^\star$ that satisfies both conditions.
4	Trim the trajectory to $\widetilde{\mathscr{P}} = \{\mathbf{x}_{i^\star}, \ldots, \mathbf{x}_{N-1}\}$, where N is the total number of frames.

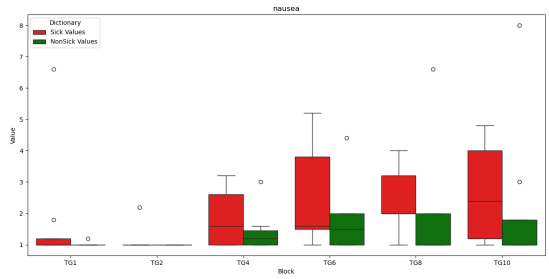

Fig. 7: Overall Nausea Results

Table 6: Workflow of the robust 3-D trajectory smoother.

Step	Operation and Definitions
1	Convert raw trajectory $\mathscr{P} = \{\mathbf{x}_0, \ldots, \mathbf{x}_{N-1}\}$ into an $N \times 3$ matrix $\mathbf{X}$, where $\mathbf{x}_i$ is the 3D position at frame i.
2	Compute speeds $v_i = \|\mathbf{x}_{i+1} - \mathbf{x}_i\|$, flag frames where $v_i > \mu_v + k_s\sigma_v$, with μ_v, σ_v the mean and standard deviation of speeds, and k_s the threshold factor.
3	Compute accelerations $a_i = \|v_{i+1} - v_i\|$, flag frames where $a_i > \mu_a + k_a\sigma_a$, with μ_a, σ_a the mean and standard deviation of accelerations, and k_a the threshold factor.
4	Replace flagged frames with `NaN`.
5	Linearly interpolate missing values for each axis (X, Y, Z).
6	Apply per-axis median filter (window size w_m).
7	Apply Savitzky–Golay filter (window w_{sg}, polynomial order d).
8	Reconstruct smoothed trajectory $\widetilde{\mathscr{P}}$, preserving original frame count.

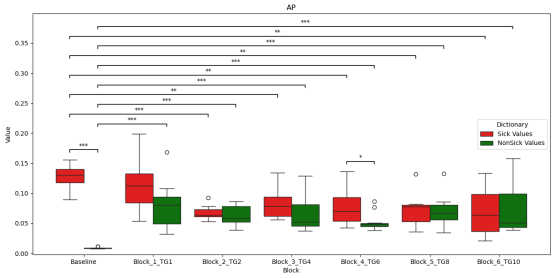

Fig. 8: Forward Box Plots.

B Box Plots and Full Statistical Results

B.1 Questionnaire Results

The full results from the statistical analysis of the questionnaire are presented in tables 7 - 9. The box plots representing these statistics can be found in figures 5 - 7.

B.2 Center of Mass Results

The full results from the statistical analysis of the Center of Mass at a spatial level can be found in tables 10 - 13. The box plots representing these statistics are displayed in figures 8 - 11.

The full results from the statistical analysis of the Center of Mass temporal dynamics can be found in tables 14 - 17. The box plots representing these statistics are displayed in figures 12 - 15.

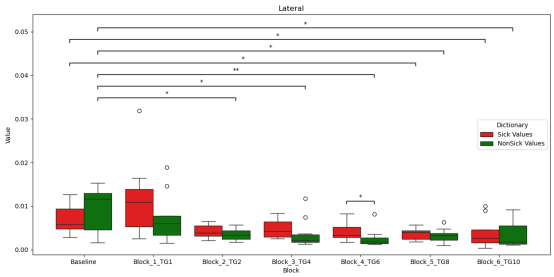

Fig. 9: Lateral Box Plots.

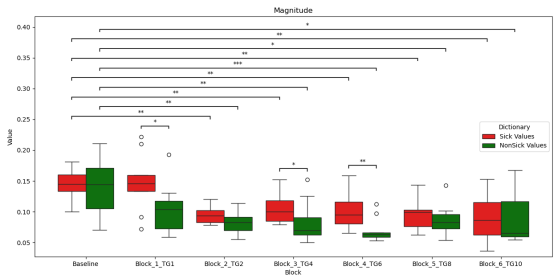

Fig. 10: Magnitude Box Plots

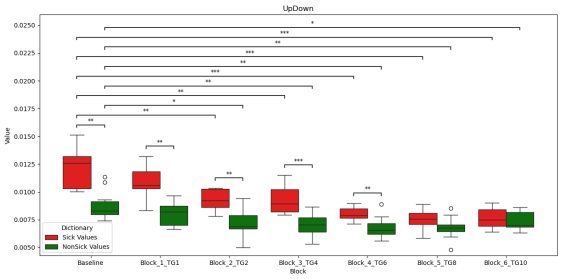

Fig. 11: Vertical Box Plots

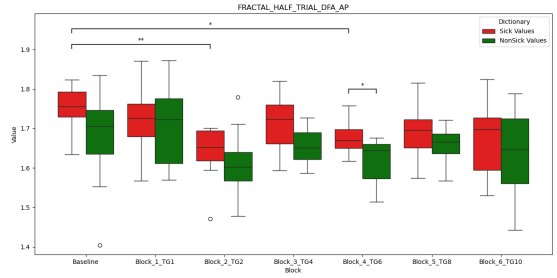

Fig. 12: Forward CoM temporal box plots.

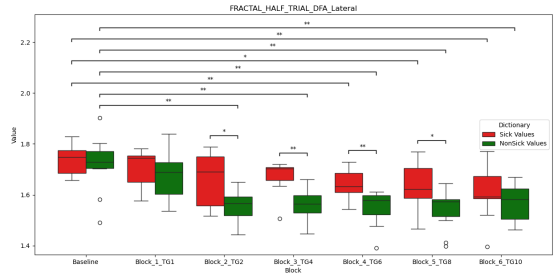

Fig. 13: Lateral CoM temporal box plots.

	Discomfort		
Block	**Statistic, p-val**	μ	σ
1	$H(14) = 0.407$, 0.524	*VRS* 2.03 *NoVRS* 1.18	1.72 0.25
2	$H(13) = 0.683$, 0.409	*VRS* 2.63 *NoVRS* 2.25	1.27 1.42
3	$H(13) = 4.927$, **0.026**	***VRS* 3.77** ***NoVRS* 1.58**	**2.14** **0.98**
4	$H(13) = 4.673$, **0.031**	***VRS* 4.40** ***NoVRS* 1.75**	**2.70** **1.30**
5	$H(11) = 1.648$, 0.199	*VRS* 3.52 *NoVRS* 1.90	2.22 1.29
6	$H(11) = 2.166$, 0.141	*VRS* 3.76 *NoVRS* 2.08	2.08 1.70

Table 7: General discomfort responses across all blocks. Significant results ($p < 0.05$) are highlighted in bold.

	Nausea		
Block	**Statistic, p-val**	μ	σ
1	$H(14) = 0.593$, 0.441	*VRS* 1.80 *NoVRS* 1.03	1.83 0.07
2	$H(13) = 1.143$, 0.285	*VRS* 1.17 *NoVRS* 1.00	0.42 0.00
3	$H(13) = 0.632$, 0.426	*VRS* 1.86 *NoVRS* 1.43	0.86 0.64
4	$H(13) = 0.998$, 0.318	*VRS* 2.63 *NoVRS* 1.80	1.53 1.06
5	$H(11) = 1.767$, 0.184	*VRS* 2.44 *NoVRS* 1.95	1.05 1.81
6	$H(11) = 1.334$, 0.248	*VRS* 2.68 *NoVRS* 2.18	1.51 2.29

Table 8: Nausea responses across all blocks.

B.3 Head Movement Results

The full results from the statistical analysis of the head movement of the spatial differences can be found in tables 18 - 21. The box plots that showcase the statistics are displayed in figures 16 - 19.

The full results from the statistical analysis of the head movement temporal dynamics can be found in tables 22 - 25. The box plots that showcase the statistics are displayed in figures 20 - 23.

C Machine Learning Results

C.1 Cross-validated Performance

The full cross-validated performance metrics for all logistic regression models are reported in tables 26–33. These tables summarize accuracy (ACC), average precision (AP), F1-score and area under the ROC curve (AUC), with results presented as mean $\pm$ standard deviation across folds.

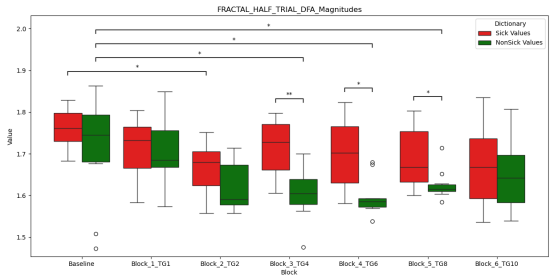

Fig. 14: Magnitudes CoM temporal box plots

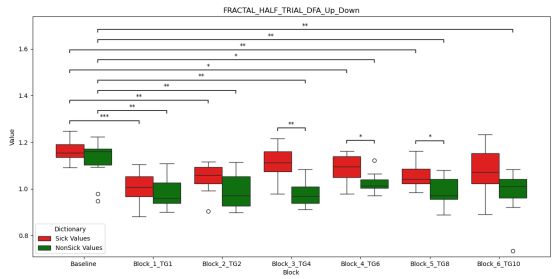

Fig. 15: Vertical CoM temporal box plots

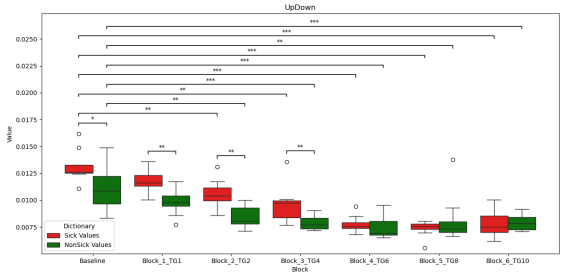

Fig. 19: Vertical Head Box Plots

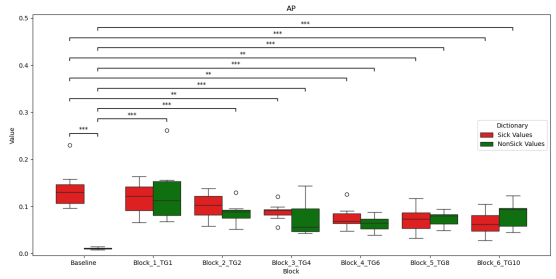

Fig. 16: Forward Head Box Plots

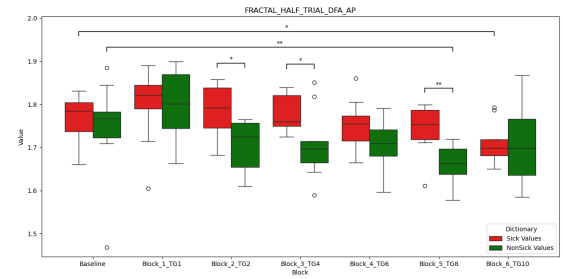

Fig. 20: Temporal dynamics of forward head movement

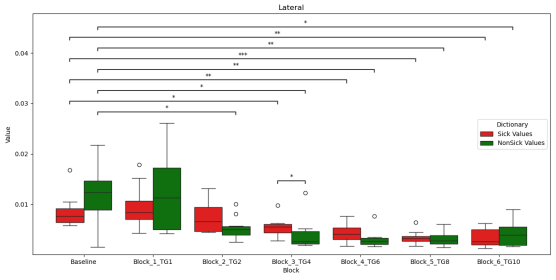

Fig. 17: Lateral Head Box Plots

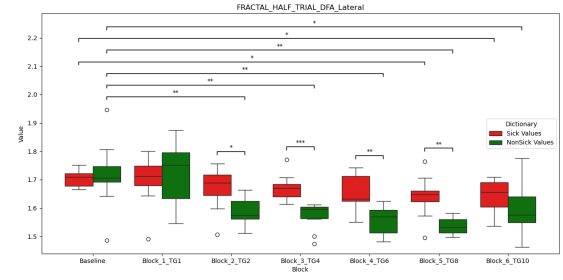

Fig. 21: Temporal dynamics of lateral head movement

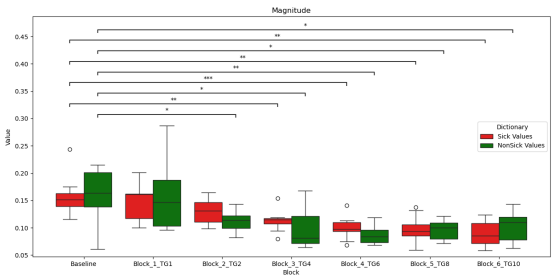

Fig. 18: Magnitude Head Box Plots

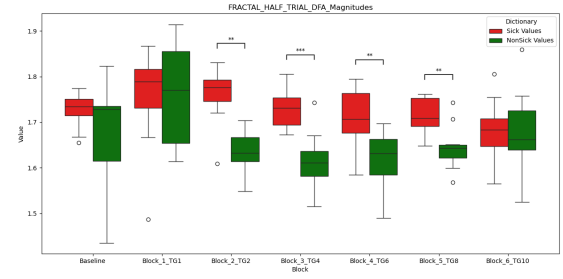

Fig. 22: Temporal dynamics of the magnitude difference of head movement

	Dizziness		
Block	**Statistic, p-val**	μ	σ
1	$H(14) = 0.028$, 0.867	*VRS* 2.03 *NoVRS* 1.43	1.91 0.64
2	$H(13) = 0.086$, 0.770	*VRS* 2.69 *NoVRS* 2.68	1.37 1.35
3	$H(13) = 0.569$, 0.451	*VRS* 3.80 *NoVRS* 2.90	1.86 1.27
4	$H(13) = 1.222$, 0.269	*VRS* 4.89 *NoVRS* 3.18	2.76 1.29
5	$H(11) = 0.659$, 0.417	*VRS* 4.28 *NoVRS* 3.30	1.82 1.62
6	$H(11) = 1.375$, 0.241	*VRS* 4.76 *NoVRS* 3.33	1.99 2.22

Table 9: Dizziness (eyes opened) responses across all blocks.

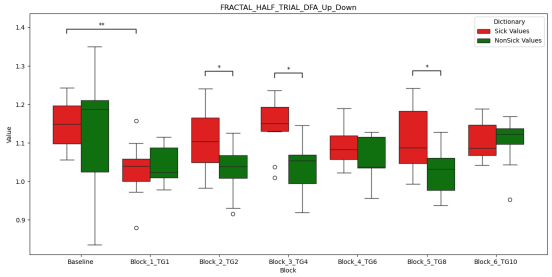

Fig. 23: Temporal dynamics of vertical head movement

Model nomenclature is as follows: `logistic_b` denotes baseline (no-VR) logistic regression models, and `logistic_e` denotes experimental (VR) variants with augmented feature sets. The suffix `_alpha_only` specifies models using only temporal DFA-based descriptors, while `_spatial_only` restricts training to spatial postural descriptors. Models without a suffix employ both feature families. The "Source" column indicates whether features originate from the head, CoM, or all available signals.

C.2 Axis-level SHAP Importances

The complete axis-level SHAP analyses are reported in tables 34–39. These tables detail the relative contributions of kinematic directions (Anterior–Posterior, Lateral, Vertical (Up–Down), and Magnitude) to model predictions across head, CoM, and combined feature sources.

Table 26: Baseline (No-VR Walking) models: meanPool results for ACC and AUC (mean ± sd).

Model	Source	ACC	AUC
logistic_b	All	0.57 ± 0.17	0.70 ± 0.23
logistic_b	CoM	0.64 ± 0.22	0.65 ± 0.39
logistic_b	Head	0.51 ± 0.13	0.50 ± 0.41
logistic_b_alpha_only	All	0.57 ± 0.05	0.63 ± 0.29
logistic_b_alpha_only	CoM	0.32 ± 0.34	0.30 ± 0.28
logistic_b_alpha_only	Head	0.46 ± 0.20	0.69 ± 0.33
logistic_b_spatial_only	All	0.57 ± 0.17	0.67 ± 0.27
logistic_b_spatial_only	CoM	0.64 ± 0.22	0.72 ± 0.28
logistic_b_spatial_only	Head	0.44 ± 0.11	0.28 ± 0.21

Table 27: Baseline (No-VR Walking) models: meanPool results for AP and F1-score (mean ± sd).

Model	Source	AP	F1-score
logistic_b	All	0.81 ± 0.14	0.59 ± 0.16
logistic_b	CoM	0.75 ± 0.25	0.53 ± 0.38
logistic_b	Head	0.69 ± 0.25	0.50 ± 0.00
logistic_b_alpha_only	All	0.73 ± 0.21	0.61 ± 0.08
logistic_b_alpha_only	CoM	0.51 ± 0.05	0.36 ± 0.33
logistic_b_alpha_only	Head	0.79 ± 0.23	0.48 ± 0.16
logistic_b_spatial_only	All	0.79 ± 0.15	0.53 ± 0.19
logistic_b_spatial_only	CoM	0.78 ± 0.21	0.53 ± 0.38
logistic_b_spatial_only	Head	0.59 ± 0.15	0.47 ± 0.05

Table 28: Baseline (No-VR Walking) models: LSE results for ACC and AUC (mean ± sd).

Model	Source	ACC	AUC
logistic_b	All	0.57 ± 0.17	0.67 ± 0.27
logistic_b	CoM	0.64 ± 0.22	0.65 ± 0.39
logistic_b	Head	0.51 ± 0.13	0.50 ± 0.41
logistic_b_alpha_only	All	0.57 ± 0.05	0.67 ± 0.24
logistic_b_alpha_only	CoM	0.32 ± 0.34	0.30 ± 0.28
logistic_b_alpha_only	Head	0.46 ± 0.20	0.69 ± 0.33
logistic_b_spatial_only	All	0.63 ± 0.26	0.74 ± 0.19
logistic_b_spatial_only	CoM	0.64 ± 0.22	0.72 ± 0.28
logistic_b_spatial_only	Head	0.44 ± 0.11	0.28 ± 0.21

Table 29: Baseline (No-VR Walking) models: LSE results for AP and F1-score (mean ± sd).

Model	Source	AP	F1-score
logistic_b	All	0.79 ± 0.15	0.62 ± 0.17
logistic_b	CoM	0.75 ± 0.25	0.53 ± 0.38
logistic_b	Head	0.69 ± 0.25	0.50 ± 0.00
logistic_b_alpha_only	All	0.75 ± 0.18	0.61 ± 0.08
logistic_b_alpha_only	CoM	0.51 ± 0.05	0.36 ± 0.33
logistic_b_alpha_only	Head	0.79 ± 0.23	0.48 ± 0.16
logistic_b_spatial_only	All	0.82 ± 0.12	0.74 ± 0.19
logistic_b_spatial_only	CoM	0.78 ± 0.21	0.53 ± 0.38
logistic_b_spatial_only	Head	0.59 ± 0.15	0.47 ± 0.05

Table 30: Experimental (VR Walking) models: meanPool results for ACC and AUC (mean ± sd).

Model	Source	ACC	AUC
logistic_e	All	0.42 ± 0.19	0.37 ± 0.32
logistic_e	CoM	0.54 ± 0.26	0.33 ± 0.24
logistic_e	Head	0.61 ± 0.18	0.56 ± 0.32
logistic_e_alpha_only	All	0.43 ± 0.17	0.26 ± 0.19
logistic_e_alpha_only	CoM	0.60 ± 0.33	0.61 ± 0.28
logistic_e_alpha_only	Head	0.38 ± 0.03	0.46 ± 0.18
logistic_e_spatial_only	All	0.57 ± 0.17	0.67 ± 0.27
logistic_e_spatial_only	CoM	0.64 ± 0.22	0.72 ± 0.28
logistic_e_spatial_only	Head	0.44 ± 0.11	0.28 ± 0.21

Spatial CoM Magnitude				
Test	**Stats**	μ	σ	**Effect Size**
[Baseline] VRS [Baseline] NoVRS	$H(16) = 0.008$ $p = 0.92920$	0.14500 0.14264	0.02360 0.04441	$\varepsilon^2 = 0.0$ 95% CI [0.0, 0.249]
[Block 1] VRS **[Block 1] NoVRS**	$H(16) = 3.947$ $p = 0.04694$	**0.14619** **0.10635**	**0.04559** **0.03887**	$\varepsilon^2 = 0.184$ **95% CI [0.0, 0.744]**
[Block 1] VRS [Baseline] VRS	$H(15) = 0.009$ $p = 0.92334$	0.14619 0.14500	0.04559 0.02360	$\varepsilon^2 = 0.0$ 95% CI [0.0, 0.265]
[Block 1] NoVRS [Baseline] NoVRS	$H(17) = 2.667$ $p = 0.10247$	0.10635 0.14264	0.03887 0.04441	$\varepsilon^2 = 0.098$ 95% CI [0.0, 0.545]
[Block 2] VRS [Block 2] NoVRS	$H(18) = 2.766$ $p = 0.09630$	0.09409 0.08215	0.01254 0.01626	$\varepsilon^2 = 0.098$ 95% CI [0.0, 0.516]
[Block 2] VRS **[Baseline] VRS**	$H(16) = 10.232$ $p = 0.00138$	**0.09409** **0.14500**	**0.01254** **0.02360**	$\varepsilon^2 = 0.577$ **95% CI [0.249, 0.742]**
[Block 2] NoVRS **[Baseline] NoVRS**	$H(18) = 9.143$ $p = 0.00250$	**0.08215** **0.14264**	**0.01626** **0.04441**	$\varepsilon^2 = 0.452$ **95% CI [0.100, 0.747]**
[Block 3] VRS **[Block 3] NoVRS**	$H(18) = 3.863$ $p = 0.04937$	**0.10418** **0.08290**	**0.02261** **0.03079**	$\varepsilon^2 = 0.159$ **95% CI [0.0, 0.650]**
[Block 3] VRS **[Baseline] VRS**	$H(16) = 7.587$ $p = 0.00588$	**0.10418** **0.14500**	**0.02261** **0.02360**	$\varepsilon^2 = 0.412$ **95% CI [0.066, 0.738]**
[Block 3] NoVRS **[Baseline] NoVRS**	$H(18) = 8.251$ $p = 0.00407$	**0.08290** **0.14264**	**0.03079** **0.04441**	$\varepsilon^2 = 0.403$ **95% CI [0.073, 0.745]**
[Block 4] VRS **[Block 4] NoVRS**	$H(18) = 7.823$ $p = 0.00516$	**0.09900** **0.06959**	**0.02707** **0.01828**	$\varepsilon^2 = 0.379$ **95% CI [0.048, 0.745]**
[Block 4] VRS **[Baseline] VRS**	$H(16) = 7.587$ $p = 0.00588$	**0.09900** **0.14500**	**0.02707** **0.02360**	$\varepsilon^2 = 0.412$ **95% CI [0.050, 0.739]**
[Block 4] NoVRS **[Baseline] NoVRS**	$H(18) = 11.571$ $p = 0.00067$	**0.06959** **0.14264**	**0.01828** **0.04441**	$\varepsilon^2 = 0.575$ **95% CI [0.232, 0.748]**
[Block 5] VRS [Block 5] NoVRS	$H(18) = 1.463$ $p = 0.22648$	0.09460 0.08572	0.02188 0.02443	$\varepsilon^2 = 0.044$ 95% CI [0.0, 0.423]
[Block 5] VRS **[Baseline] VRS**	$H(16) = 8.597$ $p = 0.00337$	**0.09460** **0.14500**	**0.02188** **0.02360**	$\varepsilon^2 = 0.475$ **95% CI [0.118, 0.740]**
[Block 5] NoVRS **[Baseline] NoVRS**	$H(18) = 6.606$ $p = 0.01017$	**0.08572** **0.14264**	**0.02443** **0.04441**	$\varepsilon^2 = 0.327$ **95% CI [0.004, 0.739]**
[Block 6] VRS [Block 6] NoVRS	$H(18) = 0.143$ $p = 0.70546$	0.09026 0.08704	0.03551 0.03799	$\varepsilon^2 = 0.0$ 95% CI [0.0, 0.252]
[Block 6] VRS **[Baseline] VRS**	$H(16) = 7.587$ $p = 0.00588$	**0.09026** **0.14500**	**0.03551** **0.02360**	$\varepsilon^2 = 0.412$ **95% CI [0.065, 0.738]**
[Block 6] NoVRS **[Baseline] NoVRS**	$H(18) = 6.606$ $p = 0.01017$	**0.08704** **0.14264**	**0.03799** **0.04441**	$\varepsilon^2 = 0.327$ **95% CI [0.005, 0.739]**

Table 10: CoM Magnitude analysis results. Significant results ($p < 0.05$) are highlighted in bold.

Spatial CoM Lateral				
Test	**Stats**	μ	σ	**Effect Size**
[Baseline] VRS [Baseline] NoVRS	$H(16) = 0.789$ $p = 0.37426$	0.00709 0.00935	0.00343 0.00469	$\varepsilon^2 = 0.019$ 95% CI [0.0, 0.388]
[Block 1] VRS [Block 1] NoVRS	$H(16) = 1.639$ $p = 0.20041$	0.01218 0.00720	0.00821 0.00556	$\varepsilon^2 = 0.061$ 95% CI [0.0, 0.527]
[Block 1] VRS [Baseline] VRS	$H(15) = 1.815$ $p = 0.17793$	0.01218 0.00709	0.00821 0.00343	$\varepsilon^2 = 0.074$ 95% CI [0.0, 0.568]
[Block 1] NoVRS [Baseline] NoVRS	$H(17) = 0.667$ $p = 0.41422$	0.00720 0.00935	0.00556 0.00469	$\varepsilon^2 = 0.0$ 95% CI [0.0, 0.376]
[Block 2] VRS [Block 2] NoVRS	$H(18) = 0.966$ $p = 0.32575$	0.00416 0.00352	0.00145 0.00128	$\varepsilon^2 = 0.020$ 95% CI [0.0, 0.412]
[Block 2] VRS [Baseline] VRS	$H(16) = 3.482$ $p = 0.06206$	0.00416 0.00709	0.00145 0.00343	$\varepsilon^2 = 0.168$ 95% CI [0.0, 0.649]
[Block 2] NoVRS **[Baseline] NoVRS**	$H(18) = 5.491$ $p = 0.01911$	**0.00352** **0.00935**	**0.00128** **0.00469**	$\varepsilon^2 = 0.275$ **95% CI [0.0, 0.712]**
[Block 3] VRS [Block 3] NoVRS	$H(18) = 3.571$ $p = 0.05878$	0.00476 0.00362	0.00201 0.00321	$\varepsilon^2 = 0.149$ 95% CI [0.0, 0.625]
[Block 3] VRS [Baseline] VRS	$H(16) = 2.282$ $p = 0.13092$	0.00476 0.00709	0.00201 0.00343	$\varepsilon^2 = 0.102$ 95% CI [0.0, 0.582]
[Block 3] NoVRS **[Baseline] NoVRS**	$H(18) = 6.606$ $p = 0.01017$	**0.00362** **0.00935**	**0.00321** **0.00469**	$\varepsilon^2 = 0.327$ **95% CI [0.0, 0.739]**
[Block 4] VRS **[Block 4] NoVRS**	$H(18) = 4.806$ $p = 0.02837$	**0.00423** **0.00258**	**0.00218** **0.00199**	$\varepsilon^2 = 0.220$ **95% CI [0.0, 0.684]**
[Block 4] VRS [Baseline] VRS	$H(16) = 2.558$ $p = 0.10974$	0.00423 0.00709	0.00218 0.00343	$\varepsilon^2 = 0.120$ 95% CI [0.0, 0.594]
[Block 4] NoVRS **[Baseline] NoVRS**	$H(18) = 8.691$ $p = 0.00320$	**0.00258** **0.00935**	**0.00199** **0.00469**	$\varepsilon^2 = 0.428$ **95% CI [0.084, 0.746]**
[Block 5] VRS [Block 5] NoVRS	$H(18) = 0.691$ $p = 0.40568$	0.00367 0.00318	0.00124 0.00153	$\varepsilon^2 = 0.0$ 95% CI [0.0, 0.371]
[Block 5] VRS **[Baseline] VRS**	$H(16) = 4.934$ $p = 0.02633$	**0.00367** **0.00709**	**0.00124** **0.00343**	$\varepsilon^2 = 0.244$ **95% CI [0.0, 0.693]**
[Block 5] NoVRS **[Baseline] NoVRS**	$H(18) = 6.223$ $p = 0.01261$	**0.00318** **0.00935**	**0.00153** **0.00469**	$\varepsilon^2 = 0.314$ **95% CI [0.023, 0.735]**
[Block 6] VRS [Block 6] NoVRS	$H(18) = 0.091$ $p = 0.76237$	0.00381 0.00366	0.00313 0.00302	$\varepsilon^2 = 0.0$ 95% CI [0.0, 0.248]
[Block 6] VRS **[Baseline] VRS**	$H(16) = 4.176$ $p = 0.04099$	**0.00381** **0.00709**	**0.00313** **0.00343**	$\varepsilon^2 = 0.205$ **95% CI [0.0, 0.671]**
[Block 6] NoVRS **[Baseline] NoVRS**	$H(18) = 6.606$ $p = 0.01017$	**0.00366** **0.00935**	**0.00302** **0.00469**	$\varepsilon^2 = 0.327$ **95% CI [0.005, 0.739]**

Table 11: Lateral analysis results. Significant results ($p < 0.05$) are highlighted in bold.

Spatial CoM Vertical				
Test	**Stats**	μ	σ	**Effect Size**
[Baseline] VRS **[Baseline] NoVRS**	$H(16) = 9.126$ $p = 0.00252$	**0.01218** **0.00876**	**0.00170** **0.00128**	$\varepsilon^2 = 0.502$ **95% CI [0.141, 0.741]**
[Block 1] VRS **[Block 1] NoVRS**	$H(16) = 10.388$ $p = 0.00127$	**0.01088** **0.00802**	**0.00132** **0.00102**	$\varepsilon^2 = 0.589$ **95% CI [0.223, 0.742]**
[Block 1] VRS [Baseline] VRS	$H(15) = 1.333$ $p = 0.24821$	0.01088 0.01218	0.00132 0.00170	$\varepsilon^2 = 0.037$ 95% CI [0.0, 0.461]
[Block 1] NoVRS [Baseline] NoVRS	$H(17) = 0.667$ $p = 0.41422$	0.00802 0.00876	0.00102 0.00128	$\varepsilon^2 = 0.0$ 95% CI [0.0, 0.376]
[Block 2] VRS **[Block 2] NoVRS**	$H(18) = 9.606$ $p = 0.00194$	**0.00928** **0.00718**	**0.00093** **0.00118**	$\varepsilon^2 = 0.482$ **95% CI [0.132, 0.740]**
[Block 2] VRS **[Baseline] VRS**	$H(16) = 8.084$ $p = 0.00447$	**0.00928** **0.01218**	**0.00093** **0.00170**	$\varepsilon^2 = 0.443$ **95% CI [0.099, 0.740]**
[Block 2] NoVRS **[Baseline] NoVRS**	$H(18) = 5.491$ $p = 0.01911$	**0.00718** **0.00876**	**0.00118** **0.00128**	$\varepsilon^2 = 0.275$ **95% CI [0.009, 0.712]**
[Block 3] VRS **[Block 3] NoVRS**	$H(18) = 11.571$ $p = 0.00067$	**0.00929** **0.00700**	**0.00123** **0.00095**	$\varepsilon^2 = 0.575$ **95% CI [0.232, 0.748]**
[Block 3] VRS **[Baseline] VRS**	$H(16) = 7.587$ $p = 0.00588$	**0.00929** **0.01218**	**0.00123** **0.00170**	$\varepsilon^2 = 0.412$ **95% CI [0.065, 0.738]**
[Block 3] NoVRS **[Baseline] NoVRS**	$H(18) = 8.251$ $p = 0.00407$	**0.00700** **0.00876**	**0.00095** **0.00128**	$\varepsilon^2 = 0.403$ **95% CI [0.073, 0.745]**
[Block 4] VRS **[Block 4] NoVRS**	$H(18) = 7.000$ $p = 0.00815$	**0.00802** **0.00683**	**0.00059** **0.00091**	$\varepsilon^2 = 0.348$ **95% CI [0.024, 0.742]**
[Block 4] VRS **[Baseline] VRS**	$H(16) = 12.632$ $p = 0.00038$	**0.00802** **0.01218**	**0.00059** **0.00170**	$\varepsilon^2 = 0.702$ **95% CI [0.343, 0.753]**
[Block 4] NoVRS **[Baseline] NoVRS**	$H(18) = 9.606$ $p = 0.00194$	**0.00683** **0.00876**	**0.00091** **0.00128**	$\varepsilon^2 = 0.482$ **95% CI [0.132, 0.740]**
[Block 5] VRS [Block 5] NoVRS	$H(18) = 3.291$ $p = 0.06964$	0.00755 0.00678	0.00085 0.00097	$\varepsilon^2 = 0.127$ 95% CI [0.0, 0.608]
[Block 5] VRS **[Baseline] VRS**	$H(16) = 12.632$ $p = 0.00038$	**0.00755** **0.01218**	**0.00085** **0.00170**	$\varepsilon^2 = 0.702$ **95% CI [0.343, 0.753]**
[Block 5] NoVRS **[Baseline] NoVRS**	$H(18) = 9.606$ $p = 0.00194$	**0.00678** **0.00876**	**0.00097** **0.00128**	$\varepsilon^2 = 0.482$ **95% CI [0.132, 0.740]**
[Block 6] VRS [Block 6] NoVRS	$H(18) = 0.463$ $p = 0.49629$	0.00763 0.00736	0.00093 0.00079	$\varepsilon^2 = 0.0$ 95% CI [0.0, 0.336]
[Block 6] VRS **[Baseline] VRS**	$H(16) = 12.632$ $p = 0.00038$	**0.00763** **0.01218**	**0.00093** **0.00170**	$\varepsilon^2 = 0.702$ **95% CI [0.343, 0.753]**
[Block 6] NoVRS **[Baseline] NoVRS**	$H(18) = 5.143$ $p = 0.02334$	**0.00736** **0.00876**	**0.00079** **0.00128**	$\varepsilon^2 = 0.258$ **95% CI [0.0, 0.706]**

Table 12: Vertical analysis results. Significant results ($p < 0.05$) are highlighted in bold.

Spatial CoM Forward				
Test	**Stats**	μ	σ	**Effect Size**
[Baseline] VRS **[Baseline] NoVRS**	$H(16) = 12.632$ $p = 0.00038$	**0.12764** **0.00876**	**0.01907** **0.00128**	$\varepsilon^2 = 0.702$ **95% CI [0.343, 0.753]**
[Block 1] VRS [Block 1] NoVRS	$H(16) = 3.604$ $p = 0.05763$	0.12053 0.08113	0.04567 0.03922	$\varepsilon^2 = 0.175$ 95% CI [0.0, 0.661]
[Block 1] VRS [Baseline] VRS	$H(15) = 0.593$ $p = 0.44142$	0.12053 0.12764	0.04567 0.01907	$\varepsilon^2 = 0.0$ 95% CI [0.0, 0.344]
[Block 1] NoVRS **[Baseline] NoVRS**	$H(17) = 13.500$ $p = 0.00024$	**0.08113** **0.00876**	**0.03922** **0.00128**	$\varepsilon^2 = 0.740$ **95% CI [0.741, 0.753]**
[Block 2] VRS [Block 2] NoVRS	$H(18) = 0.463$ $p = 0.49629$	0.06716 0.06310	0.01133 0.01569	$\varepsilon^2 = 0.0$ 95% CI [0.0, 0.336]
[Block 2] VRS **[Baseline] VRS**	$H(16) = 12.008$ $p = 0.00053$	**0.06716** **0.12764**	**0.01133** **0.01907**	$\varepsilon^2 = 0.677$ **95% CI [0.303, 0.752]**
[Block 2] NoVRS **[Baseline] NoVRS**	$H(18) = 14.286$ $p = 0.00016$	**0.06310** **0.00876**	**0.01569** **0.00128**	$\varepsilon^2 = 0.738$ **95% CI [0.740, 0.753]**
[Block 3] VRS [Block 3] NoVRS	$H(18) = 2.520$ $p = 0.11241$	0.08115 0.06619	0.02325 0.02861	$\varepsilon^2 = 0.084$ 95% CI [0.0, 0.539]
[Block 3] VRS **[Baseline] VRS**	$H(16) = 8.597$ $p = 0.00337$	**0.08115** **0.12764**	**0.02325** **0.01907**	$\varepsilon^2 = 0.475$ **95% CI [0.118, 0.740]**
[Block 3] NoVRS **[Baseline] NoVRS**	$H(18) = 14.286$ $p = 0.00016$	**0.06619** **0.00876**	**0.02861** **0.00128**	$\varepsilon^2 = 0.738$ **95% CI [0.741, 0.753]**
[Block 4] VRS **[Block 4] NoVRS**	$H(18) = 3.863$ $p = 0.04937$	**0.07598** **0.05302**	**0.02789** **0.01468**	$\varepsilon^2 = 0.159$ **95% CI [0.0, 0.620]**
[Block 4] VRS **[Baseline] VRS**	$H(16) = 8.597$ $p = 0.00337$	**0.07598** **0.12764**	**0.02789** **0.01907**	$\varepsilon^2 = 0.475$ **95% CI [0.118, 0.740]**
[Block 4] NoVRS **[Baseline] NoVRS**	$H(18) = 14.286$ $p = 0.00016$	**0.05302** **0.00876**	**0.01468** **0.00128**	$\varepsilon^2 = 0.738$ **95% CI [0.741, 0.754]**
[Block 5] VRS [Block 5] NoVRS	$H(18) = 0.023$ $p = 0.87983$	0.07232 0.06982	0.02520 0.02602	$\varepsilon^2 = 0.0$ 95% CI [0.0, 0.252]
[Block 5] VRS **[Baseline] VRS**	$H(16) = 9.671$ $p = 0.00187$	**0.07232** **0.12764**	**0.02520** **0.01907**	$\varepsilon^2 = 0.542$ **95% CI [0.179, 0.742]**
[Block 5] NoVRS **[Baseline] NoVRS**	$H(18) = 14.286$ $p = 0.00016$	**0.06982** **0.00876**	**0.02602** **0.00128**	$\varepsilon^2 = 0.738$ **95% CI [0.741, 0.753]**
[Block 6] VRS [Block 6] NoVRS	$H(18) = 0.143$ $p = 0.70546$	0.06854 0.07197	0.03717 0.03926	$\varepsilon^2 = 0.0$ 95% CI [0.0, 0.253]
[Block 6] VRS **[Baseline] VRS**	$H(16) = 8.084$ $p = 0.00447$	**0.06854** **0.12764**	**0.03717** **0.01907**	$\varepsilon^2 = 0.443$ **95% CI [0.099, 0.740]**
[Block 6] NoVRS **[Baseline] NoVRS**	$H(18) = 14.286$ $p = 0.00016$	**0.07197** **0.00876**	**0.03926** **0.00128**	$\varepsilon^2 = 0.738$ **95% CI [0.741, 0.753]**

Table 13: Forward analysis results. Significant results ($p < 0.05$) are highlighted in bold.

Temporal CoM Magnitude				
Test	**Stats**	μ	σ	**Updated Effect Size**
[Baseline] VRS [Baseline] NoVRS	H(16) = 0.197 $p = 0.65685$	1.75884 1.71289	0.04909 0.12571	$\varepsilon^2 = 0.0$ 95% CI [0.0, 0.277]
[Block 1] VRS [Block 1] NoVRS	H(16) = 0.049 $p = 0.82528$	1.71122 1.70624	0.06747 0.07858	$\varepsilon^2 = 0.0$ 95% CI [0.0, 0.265]
[Baseline] VRS [Block 1] VRS	H(15) = 2.083 $p = 0.14891$	1.75884 1.71122	0.04909 0.06747	$\varepsilon^2 = 0.075$ 95% CI [0.0, 0.540]
[Baseline] NoVRS [Block 1] NoVRS	H(17) = 0.540 $p = 0.46243$	1.71289 1.70624	0.12571 0.07858	$\varepsilon^2 = 0.0$ 95% CI [0.0, 0.384]
[Block 2] VRS [Block 2] NoVRS	H(18) = 2.063 $p = 0.15093$	1.66791 1.61779	0.06216 0.05689	$\varepsilon^2 = 0.063$ 95% CI [0.0, 0.466]
[Baseline] VRS **[Block 2] VRS**	**H(16) = 5.755** $p = 0.01644$	**1.75884** **1.66791**	**0.04909** **0.06216**	$\varepsilon^2 = 0.297$ **95% CI [0.0, 0.694]**
[Baseline] NoVRS [Block 2] NoVRS	$H(18) = 3.291$ $p = 0.06964$	1.71289 1.61779	0.12571 0.05689	$\varepsilon^2 = 0.131$ 95% CI [0.0, 0.551]
[Block 3] VRS **[Block 3] NoVRS**	**H(18) = 8.691** $p = 0.00320$	**1.71509** **1.60702**	**0.06158** **0.06018**	$\varepsilon^2 = 0.427$ **95% CI [0.099, 0.745]**
[Baseline] VRS [Block 3] VRS	H(16) = 2.282 $p = 0.13092$	1.75884 1.71509	0.04909 0.06158	$\varepsilon^2 = 0.080$ 95% CI [0.0, 0.511]
[Baseline] NoVRS **[Block 3] NoVRS**	**H(18) = 4.480** $p = 0.03429$	**1.71289** **1.60702**	**0.12571** **0.06018**	$\varepsilon^2 = 0.193$ **95% CI [0.0, 0.621]**
[Block 4] VRS **[Block 4] NoVRS**	**H(18) = 6.223** $p = 0.01261$	**1.69644** **1.59691**	**0.08101** **0.04307**	$\varepsilon^2 = 0.290$ **95% CI [0.0, 0.669]**
[Baseline] VRS [Block 4] VRS	H(16) = 2.558 $p = 0.10974$	1.75884 1.69644	0.04909 0.08101	$\varepsilon^2 = 0.097$ 95% CI [0.0, 0.536]
[Baseline] NoVRS **[Block 4] NoVRS**	**H(18) = 4.806** $p = 0.02837$	**1.71289** **1.59691**	**0.12571** **0.04307**	$\varepsilon^2 = 0.211$ **95% CI [0.0, 0.628]**
[Block 5] VRS **[Block 5] NoVRS**	**H(18) = 4.480** $p = 0.03429$	**1.68846** **1.62553**	**0.06892** **0.03370**	$\varepsilon^2 = 0.193$ **95% CI [0.0, 0.613]**
[Baseline] VRS [Block 5] VRS	H(16) = 3.482 $p = 0.06206$	1.75884 1.68846	0.04909 0.06892	$\varepsilon^2 = 0.155$ 95% CI [0.0, 0.587]
[Baseline] NoVRS **[Block 5] NoVRS**	**H(18) = 4.480** $p = 0.03429$	**1.71289** **1.62553**	**0.12571** **0.03370**	$\varepsilon^2 = 0.193$ **95% CI [0.0, 0.623]**
[Block 6] VRS [Block 6] NoVRS	H(18) = 0.051 $p = 0.82060$	1.66992 1.64776	0.09396 0.07986	$\varepsilon^2 = 0.0$ 95% CI [0.0, 0.231]
[Baseline] VRS [Block 6] VRS	H(16) = 3.821 $p = 0.05061$	1.75884 1.66992	0.04909 0.09396	$\varepsilon^2 = 0.176$ 95% CI [0.0, 0.610]
[Baseline] NoVRS [Block 6] NoVRS	H(18) = 1.651 $p = 0.19876$	1.71289 1.64776	0.12571 0.07986	$\varepsilon^2 = 0.036$ 95% CI [0.0, 0.395]

Table 14: Magnitude analysis results. Significant results ($p < 0.05$) are highlighted in bold.

Temporal CoM Lateral				
Test	**Stats**	μ	σ	**Updated Effect Size**
[Baseline] VRS [Baseline] NoVRS	H(16) = 0.032 $p = 0.85895$	1.73600 1.71795	0.05689 0.10824	$\varepsilon^2 = 0.0$ 95% CI [0.0, 0.253]
[Block 1] VRS [Block 1] NoVRS	H(16) = 0.563 $p = 0.45291$	1.70975 1.68370	0.06995 0.09526	$\varepsilon^2 = 0.0$ 95% CI [0.0, 0.380]
[Baseline] VRS [Block 1] VRS	H(15) = 0.454 $p = 0.50058$	1.73600 1.70975	0.05689 0.06995	$\varepsilon^2 = 0.0$ 95% CI [0.0, 0.435]
[Baseline] NoVRS [Block 1] NoVRS	H(17) = 0.807 $p = 0.36911$	1.71795 1.68370	0.10824 0.09526	$\varepsilon^2 = 0.0$ 95% CI [0.0, 0.457]
[Block 2] VRS **[Block 2] NoVRS**	**H(18) = 4.480** $p = 0.03429$	**1.66071** **1.55836**	**0.09948** **0.05779**	$\varepsilon^2 = 0.193$ **95% CI [0.0, 0.621]**
[Baseline] VRS [Block 2] VRS	H(16) = 2.021 $p = 0.15513$	1.73600 1.66071	0.05689 0.09948	$\varepsilon^2 = 0.064$ 95% CI [0.0, 0.485]
[Baseline] NoVRS **[Block 2] NoVRS**	**H(18) = 7.823** $p = 0.00516$	**1.71795** **1.55836**	**0.10824** **0.05779**	$\varepsilon^2 = 0.379$ **95% CI [0.026, 0.748]**
[Block 3] VRS **[Block 3] NoVRS**	**H(18) = 8.251** $p = 0.00407$	**1.67141** **1.56676**	**0.06137** **0.06059**	$\varepsilon^2 = 0.403$ **95% CI [0.055, 0.739]**
[Baseline] VRS [Block 3] VRS	H(16) = 3.158 $p = 0.07556$	1.73600 1.67141	0.05689 0.06137	$\varepsilon^2 = 0.135$ 95% CI [0.0, 0.584]
[Baseline] NoVRS **[Block 3] NoVRS**	**H(18) = 7.823** $p = 0.00516$	**1.71795** **1.56676**	**0.10824** **0.06059**	$\varepsilon^2 = 0.379$ **95% CI [0.027, 0.730]**
[Block 4] VRS **[Block 4] NoVRS**	**H(18) = 7.823** $p = 0.00516$	**1.63986** **1.54773**	**0.05741** **0.06735**	$\varepsilon^2 = 0.379$ **95% CI [0.026, 0.741]**
[Baseline] VRS **[Block 4] VRS**	**H(16) = 7.105** $p = 0.00769$	**1.73600** **1.63986**	**0.05689** **0.05741**	$\varepsilon^2 = 0.382$ **95% CI [0.036, 0.735]**
[Baseline] NoVRS **[Block 4] NoVRS**	**H(18) = 7.823** $p = 0.00516$	**1.71795** **1.54773**	**0.10824** **0.06735**	$\varepsilon^2 = 0.379$ **95% CI [0.023, 0.737]**
[Block 5] VRS **[Block 5] NoVRS**	**H(18) = 4.480** $p = 0.03429$	**1.63379** **1.54492**	**0.09207** **0.07885**	$\varepsilon^2 = 0.193$ **95% CI [0.0, 0.613]**
[Baseline] VRS **[Block 5] VRS**	**H(16) = 4.934** $p = 0.02633$	**1.73600** **1.63379**	**0.05689** **0.09207**	$\varepsilon^2 = 0.246$ **95% CI [0.0, 0.671]**
[Baseline] NoVRS **[Block 5] NoVRS**	**H(18) = 8.691** $p = 0.00320$	**1.71795** **1.54492**	**0.10824** **0.07885**	$\varepsilon^2 = 0.427$ **95% CI [0.082, 0.751]**
[Block 6] VRS [Block 6] NoVRS	H(18) = 0.691 $p = 0.40568$	1.61121 1.56743	0.10487 0.06986	$\varepsilon^2 = 0.0$ 95% CI [0.0, 0.354]
[Baseline] VRS **[Block 6] VRS**	**H(16) = 6.639** $p = 0.00997$	**1.73600** **1.61121**	**0.05689** **0.10487**	$\varepsilon^2 = 0.352$ **95% CI [0.015, 0.729]**
[Baseline] NoVRS **[Block 6] NoVRS**	**H(18) = 7.823** $p = 0.00516$	**1.71795** **1.56743**	**0.10824** **0.06986**	$\varepsilon^2 = 0.379$ **95% CI [0.024, 0.734]**

Table 15: Lateral analysis results. Significant results ($p < 0.05$) are highlighted in bold.

Temporal CoM Vertical				
Test	**Stats**	μ	σ	**Updated Effect Size**
[Baseline] VRS [Baseline] NoVRS	H(16) = 0.197 $p = 0.65685$	1.16256 1.12091	0.04613 0.08525	$\varepsilon^2 = 0.0$ 95% CI [0.0, 0.285]
[Block 1] VRS [Block 1] NoVRS	H(16) = 0.439 $p = 0.50780$	1.00393 0.98489	0.06167 0.06565	$\varepsilon^2 = 0.0$ 95% CI [0.0, 0.354]
[Baseline] VRS **[Block 1] VRS**	**H(15) = 11.343** $p = 0.00076$	**1.16256** **1.00393**	**0.04613** **0.06167**	$\varepsilon^2 = 0.690$ **95% CI [0.301, 0.880]**
[Baseline] NoVRS **[Block 1] NoVRS**	**H(17) = 7.707** $p = 0.00550$	**1.12091** **0.98489**	**0.08525** **0.06565**	$\varepsilon^2 = 0.421$ **95% CI [0.065, 0.778]**
[Block 2] VRS [Block 2] NoVRS	H(18) = 3.291 $p = 0.06964$	1.04871 0.98773	0.06199 0.07392	$\varepsilon^2 = 0.127$ 95% CI [0.0, 0.551]
[Baseline] VRS **[Block 2] VRS**	**H(16) = 10.808** $p = 0.00101$	**1.16256** **1.04871**	**0.04613** **0.06199**	$\varepsilon^2 = 0.654$ **95% CI [0.283, 0.875]**
[Baseline] NoVRS **[Block 2] NoVRS**	**H(18) = 8.251** $p = 0.00407$	**1.12091** **0.98773**	**0.08525** **0.07392**	$\varepsilon^2 = 0.403$ **95% CI [0.062, 0.731]**
[Block 3] VRS **[Block 3] NoVRS**	**H(18) = 9.606** $p = 0.00194$	**1.10861** **0.98360**	**0.07395** **0.05753**	$\varepsilon^2 = 0.478$ **95% CI [0.128, 0.793]**
[Baseline] VRS [Block 3] VRS	H(16) = 1.776 $p = 0.18260$	1.16256 1.10861	0.04613 0.07395	$\varepsilon^2 = 0.048$ 95% CI [0.0, 0.441]
[Baseline] NoVRS **[Block 3] NoVRS**	**H(18) = 9.143** $p = 0.00250$	**1.12091** **0.98360**	**0.08525** **0.05753**	$\varepsilon^2 = 0.452$ **95% CI [0.091, 0.767]**
[Block 4] VRS **[Block 4] NoVRS**	**H(18) = 6.606** $p = 0.01017$	**1.08859** **1.02322**	**0.05580** **0.04197**	$\varepsilon^2 = 0.311$ **95% CI [0.0, 0.697]**
[Baseline] VRS **[Block 4] VRS**	**H(16) = 5.755** $p = 0.01644$	**1.16256** **1.08859**	**0.04613** **0.05580**	$\varepsilon^2 = 0.297$ **95% CI [0.0, 0.672]**
[Baseline] NoVRS **[Block 4] NoVRS**	**H(18) = 5.143** $p = 0.02334$	**1.12091** **1.02322**	**0.08525** **0.04197**	$\varepsilon^2 = 0.230$ **95% CI [0.0, 0.635]**
[Block 5] VRS **[Block 5] NoVRS**	**H(18) = 5.143** $p = 0.02334$	**1.05868** **0.99106**	**0.05448** **0.06091**	$\varepsilon^2 = 0.230$ **95% CI [0.0, 0.634]**
[Baseline] VRS **[Block 5] VRS**	**H(16) = 8.597** $p = 0.00337$	**1.16256** **1.05868**	**0.04613** **0.05448**	$\varepsilon^2 = 0.475$ **95% CI [0.106, 0.796]**
[Baseline] NoVRS **[Block 5] NoVRS**	**H(18) = 8.251** $p = 0.00407$	**1.12091** **0.99106**	**0.08525** **0.06091**	$\varepsilon^2 = 0.403$ **95% CI [0.059, 0.742]**
[Block 6] VRS [Block 6] NoVRS	H(18) = 3.571 $p = 0.05878$	1.08243 0.98312	0.09900 0.09535	$\varepsilon^2 = 0.143$ 95% CI [0.0, 0.551]
[Baseline] VRS [Block 6] VRS	H(16) = 2.850 $p = 0.09137$	1.16256 1.08243	0.04613 0.09900	$\varepsilon^2 = 0.116$ 95% CI [0.0, 0.590]
[Baseline] NoVRS **[Block 6] NoVRS**	**H(18) = 7.000** $p = 0.00815$	**1.12091** **0.98312**	**0.08525** **0.09535**	$\varepsilon^2 = 0.333$ **95% CI [0.0, 0.710]**

Table 16: Vertical analysis results. Significant results ($p < 0.05$) are highlighted in bold.

Temporal CoM Forward				
Test	**Stats**	μ	σ	**Updated Effect Size**
[Baseline] VRS [Baseline] NoVRS	H(16) = 1.547 $p = 0.21352$	1.75159 1.67700	0.05780 0.11857	$\varepsilon^2 = 0.034$ 95% CI [0.0, 0.449]
[Block 1] VRS [Block 1] NoVRS	H(16) = 0.002 $p = 0.96478$	1.72251 1.70078	0.07962 0.10042	$\varepsilon^2 = 0.0$ 95% CI [0.0, 0.252]
[Baseline] VRS [Block 1] VRS	H(15) = 1.120 $p = 0.28984$	1.75159 1.72251	0.05780 0.07962	$\varepsilon^2 = 0.008$ 95% CI [0.0, 0.428]
[Baseline] NoVRS [Block 1] NoVRS	H(17) = 0.060 $p = 0.80650$	1.67700 1.70078	0.11857 0.10042	$\varepsilon^2 = 0.0$ 95% CI [0.0, 0.316]
[Block 2] VRS [Block 2] NoVRS	H(18) = 1.120 $p = 0.28992$	1.63943 1.61493	0.06755 0.07971	$\varepsilon^2 = 0.007$ 95% CI [0.0, 0.395]
[Baseline] VRS **[Block 2] VRS**	**H(16) = 9.671** $p = 0.00187$	**1.75159** **1.63943**	**0.05780** **0.06755**	$\varepsilon^2 = 0.542$ **95% CI [0.155, 0.825]**
[Baseline] NoVRS [Block 2] NoVRS	H(18) = 2.063 $p = 0.15093$	1.67700 1.61493	0.11857 0.07971	$\varepsilon^2 = 0.059$ 95% CI [0.0, 0.457]
[Block 3] VRS [Block 3] NoVRS	t(18) = 2.068 $p = 0.05328$	1.71278 1.65420	0.07288 0.04367	$\varepsilon^2 = 0.192$ 95% CI [0.0, 0.584]
[Baseline] VRS [Block 3] VRS	H(16) = 1.334 $p = 0.24806$	1.75159 1.71278	0.05780 0.07288	$\varepsilon^2 = 0.021$ 95% CI [0.0, 0.419]
[Baseline] NoVRS [Block 3] NoVRS	H(18) = 1.463 $p = 0.22648$	1.67700 1.65420	0.11857 0.04367	$\varepsilon^2 = 0.026$ 95% CI [0.0, 0.421]
[Block 4] VRS **[Block 4] NoVRS**	**H(18) = 3.863** $p = 0.04937$	**1.67623** **1.61508**	**0.04083** **0.05749**	$\varepsilon^2 = 0.159$ **95% CI [0.0, 0.569]**
[Baseline] VRS **[Block 4] VRS**	**H(16) = 6.189** $p = 0.01285$	**1.75159** **1.67623**	**0.05780** **0.04083**	$\varepsilon^2 = 0.324$ **95% CI [0.0, 0.697]**
[Baseline] NoVRS [Block 4] NoVRS	H(18) = 3.291 $p = 0.06964$	1.67700 1.61508	0.11857 0.05749	$\varepsilon^2 = 0.127$ 95% CI [0.0, 0.533]
[Block 5] VRS [Block 5] NoVRS	H(18) = 1.851 $p = 0.17362$	1.69302 1.65592	0.06817 0.04868	$\varepsilon^2 = 0.047$ 95% CI [0.0, 0.457]
[Baseline] VRS [Block 5] VRS	H(16) = 3.158 $p = 0.07556$	1.75159 1.69302	0.05780 0.06817	$\varepsilon^2 = 0.135$ 95% CI [0.0, 0.592]
[Baseline] NoVRS [Block 5] NoVRS	H(18) = 1.120 $p = 0.28992$	1.67700 1.65592	0.11857 0.04868	$\varepsilon^2 = 0.007$ 95% CI [0.0, 0.395]
[Block 6] VRS [Block 6] NoVRS	H(18) = 0.091 $p = 0.76237$	1.67248 1.64228	0.09519 0.11199	$\varepsilon^2 = 0.0$ 95% CI [0.0, 0.316]
[Baseline] VRS [Block 6] VRS	H(16) = 2.850 $p = 0.09137$	1.75159 1.67248	0.05780 0.09519	$\varepsilon^2 = 0.116$ 95% CI [0.0, 0.551]
[Baseline] NoVRS [Block 6] NoVRS	H(18) = 0.463 $p = 0.49629$	1.67700 1.64228	0.11857 0.11199	$\varepsilon^2 = 0.0$ 95% CI [0.0, 0.334]

Table 17: Forward analysis results. Significant results ($p < 0.05$) are highlighted in bold.

Spatial Head Movement Magnitude				
Test	**Stats**	μ	σ	**Updated Effect Size**
[Baseline] VRS [Baseline] NoVRS	H(16) = 0.008 $p = 0.92920$	0.15793 0.15799	0.03710 0.05002	$\varepsilon^2 = 0.0$ 95% CI [0.0, 0.275]
[Block 1] VRS [Block 1] NoVRS	H(16) = 0.049 $p = 0.82528$	0.14845 0.15493	0.03262 0.05885	$\varepsilon^2 = 0.0$ 95% CI [0.0, 0.284]
[Block 1] VRS [Baseline] VRS	H(15) = 0.000 $p = 1.00000$	0.14845 0.15793	0.03262 0.03710	$\varepsilon^2 = 0.0$ 95% CI [0.0, 0.292]
[Block 1] NoVRS [Baseline] NoVRS	H(17) = 0.167 $p = 0.68309$	0.15493 0.15799	0.05885 0.05002	$\varepsilon^2 = 0.0$ 95% CI [0.0, 0.297]
[Block 2] VRS [Block 2] NoVRS	H(18) = 3.291 $p = 0.06964$	0.12971 0.11140	0.02143 0.01673	$\varepsilon^2 = 0.127$ 95% CI [0.0, 0.542]
[Block 2] VRS [Baseline] VRS	H(16) = 3.158 $p = 0.07556$	0.12971 0.15793	0.02143 0.03710	$\varepsilon^2 = 0.135$ 95% CI [0.0, 0.586]
[Block 2] NoVRS **[Baseline] NoVRS**	**H(18) = 4.480** $p = 0.03429$	**0.11140** **0.15799**	**0.01673** **0.05002**	$\varepsilon^2 = 0.193$ **95% CI [0.0, 0.745]**
[Block 3] VRS [Block 3] NoVRS	H(18) = 1.851 $p = 0.17362$	0.11268 0.09674	0.01801 0.03340	$\varepsilon^2 = 0.047$ 95% CI [0.0, 0.510]
[Block 3] VRS **[Baseline] VRS**	**H(16) = 9.126** $p = 0.00252$	**0.11268** **0.15793**	**0.01801** **0.03710**	$\varepsilon^2 = 0.508$ **95% CI [0.179, 0.740]**
[Block 3] NoVRS **[Baseline] NoVRS**	**H(18) = 6.223** $p = 0.01261$	**0.09674** **0.15799**	**0.03340** **0.05002**	$\varepsilon^2 = 0.290$ **95% CI [0.0, 0.746]**
[Block 4] VRS [Block 4] NoVRS	H(18) = 2.520 $p = 0.11241$	0.09995 0.08671	0.01941 0.01579	$\varepsilon^2 = 0.084$ 95% CI [0.0, 0.512]
[Block 4] VRS **[Baseline] VRS**	**H(16) = 11.400** $p = 0.00073$	**0.09995** **0.15793**	**0.01941** **0.03710**	$\varepsilon^2 = 0.650$ **95% CI [0.418, 0.743]**
[Block 4] NoVRS **[Baseline] NoVRS**	**H(18) = 7.406** $p = 0.00650$	**0.08671** **0.15799**	**0.01579** **0.05002**	$\varepsilon^2 = 0.356$ **95% CI [0.007, 0.748]**
[Block 5] VRS [Block 5] NoVRS	H(18) = 0.091 $p = 0.76237$	0.09678 0.09660	0.02272 0.01727	$\varepsilon^2 = 0.0$ 95% CI [0.0, 0.253]
[Block 5] VRS **[Baseline] VRS**	**H(16) = 10.232** $p = 0.00138$	**0.09678** **0.15793**	**0.02272** **0.03710**	$\varepsilon^2 = 0.577$ **95% CI [0.251, 0.741]**
[Block 5] NoVRS **[Baseline] NoVRS**	**H(18) = 6.223** $p = 0.01261$	**0.09660** **0.15799**	**0.01727** **0.05002**	$\varepsilon^2 = 0.290$ **95% CI [0.0, 0.748]**
[Block 6] VRS [Block 6] NoVRS	H(18) = 0.823 $p = 0.36435$	0.08935 0.10129	0.02168 0.02522	$\varepsilon^2 = 0.0$ 95% CI [0.0, 0.360]
[Block 6] VRS **[Baseline] VRS**	**H(16) = 10.808** $p = 0.00101$	**0.08935** **0.15793**	**0.02168** **0.03710**	$\varepsilon^2 = 0.613$ **95% CI [0.356, 0.742]**
[Block 6] NoVRS **[Baseline] NoVRS**	**H(18) = 5.491** $p = 0.01911$	**0.10129** **0.15799**	**0.02522** **0.05002**	$\varepsilon^2 = 0.250$ **95% CI [0.0, 0.744]**

Table 18: Magnitude analysis results. Significant results ($p < 0.05$) are highlighted in bold.

Spatial Head Movement Lateral				
Test	**Stats**	μ	σ	**Updated Effect Size**
[Baseline] VRS [Baseline] NoVRS	H(16) = 1.547 $p = 0.21352$	0.00868 0.01141	0.00339 0.00575	$\varepsilon^2 = 0.034$ 95% CI [0.0, 0.446]
[Block 1] VRS [Block 1] NoVRS	H(16) = 0.158 $p = 0.69110$	0.00947 0.01206	0.00418 0.00729	$\varepsilon^2 = 0.0$ 95% CI [0.0, 0.315]
[Block 1] VRS [Baseline] VRS	H(15) = 0.148 $p = 0.70031$	0.00947 0.00868	0.00418 0.00339	$\varepsilon^2 = 0.0$ 95% CI [0.0, 0.320]
[Block 1] NoVRS [Baseline] NoVRS	H(17) = 0.060 $p = 0.80650$	0.01206 0.01141	0.00729 0.00575	$\varepsilon^2 = 0.0$ 95% CI [0.0, 0.287]
[Block 2] VRS [Block 2] NoVRS	H(18) = 1.463 $p = 0.22648$	0.00740 0.00531	0.00302 0.00212	$\varepsilon^2 = 0.026$ 95% CI [0.0, 0.444]
[Block 2] VRS [Baseline] VRS	H(16) = 0.789 $p = 0.37426$	0.00740 0.00868	0.00302 0.00339	$\varepsilon^2 = 0.0$ 95% CI [0.0, 0.395]
[Block 2] NoVRS **[Baseline] NoVRS**	**H(18) = 4.806** $p = 0.02837$	**0.00531** **0.01141**	**0.00212** **0.00575**	$\varepsilon^2 = 0.211$ **95% CI [0.0, 0.745]**
[Block 3] VRS **[Block 3] NoVRS**	**H(18) = 5.143** $p = 0.02334$	**0.00541** **0.00391**	**0.00181** **0.00301**	$\varepsilon^2 = 0.230$ **95% CI [0.0, 0.744]**
[Block 3] VRS **[Baseline] VRS**	**H(16) = 5.755** $p = 0.01644$	**0.00541** **0.00868**	**0.00181** **0.00339**	$\varepsilon^2 = 0.297$ **95% CI [0.0, 0.733]**
[Block 3] NoVRS **[Baseline] NoVRS**	**H(18) = 6.223** $p = 0.01261$	**0.00391** **0.01141**	**0.00301** **0.00575**	$\varepsilon^2 = 0.290$ **95% CI [0.0, 0.748]**
[Block 4] VRS [Block 4] NoVRS	H(18) = 2.766 $p = 0.09630$	0.00428 0.00304	0.00181 0.00167	$\varepsilon^2 = 0.098$ 95% CI [0.0, 0.518]
[Block 4] VRS **[Baseline] VRS**	**H(16) = 9.126** $p = 0.00252$	**0.00428** **0.00868**	**0.00181** **0.00339**	$\varepsilon^2 = 0.508$ **95% CI [0.179, 0.741]**
[Block 4] NoVRS **[Baseline] NoVRS**	**H(18) = 7.000** $p = 0.00815$	**0.00304** **0.01141**	**0.00167** **0.00575**	$\varepsilon^2 = 0.333$ **95% CI [0.0, 0.748]**
[Block 5] VRS [Block 5] NoVRS	H(18) = 0.143 $p = 0.70546$	0.00335 0.00328	0.00125 0.00153	$\varepsilon^2 = 0.0$ 95% CI [0.0, 0.283]
[Block 5] VRS **[Baseline] VRS**	**H(16) = 11.400** $p = 0.00073$	**0.00335** **0.00868**	**0.00125** **0.00339**	$\varepsilon^2 = 0.650$ **95% CI [0.418, 0.742]**
[Block 5] NoVRS **[Baseline] NoVRS**	**H(18) = 7.823** $p = 0.00516$	**0.00328** **0.01141**	**0.00153** **0.00575**	$\varepsilon^2 = 0.379$ **95% CI [0.026, 0.746]**
[Block 6] VRS [Block 6] NoVRS	H(18) = 0.463 $p = 0.49629$	0.00332 0.00411	0.00185 0.00232	$\varepsilon^2 = 0.0$ 95% CI [0.0, 0.329]
[Block 6] VRS **[Baseline] VRS**	**H(16) = 10.232** $p = 0.00138$	**0.00332** **0.00868**	**0.00185** **0.00339**	$\varepsilon^2 = 0.577$ **95% CI [0.251, 0.740]**
[Block 6] NoVRS **[Baseline] NoVRS**	**H(18) = 6.223** $p = 0.01261$	**0.00411** **0.01141**	**0.00232** **0.00575**	$\varepsilon^2 = 0.290$ **95% CI [0.0, 0.747]**

Table 19: Lateral analysis results. Significant results ($p < 0.05$) are highlighted in bold.

Spatial Head Movement Vertical				
Test	**Stats**	μ	σ	**Updated Effect Size**
[Baseline] VRS **[Baseline] NoVRS**	**H(16) = 4.547** $p = 0.03297$	**0.01313** **0.01119**	**0.00150** **0.00197**	$\varepsilon^2 = 0.222$ **95% CI [0.0, 0.743]**
[Block 1] VRS **[Block 1] NoVRS**	**H(16) = 7.253** $p = 0.00708$	**0.01172** **0.00985**	**0.00101** **0.00120**	$\varepsilon^2 = 0.391$ **95% CI [0.046, 0.742]**
[Block 1] VRS [Baseline] VRS	H(15) = 3.343 $p = 0.06751$	0.01172 0.01313	0.00101 0.00150	$\varepsilon^2 = 0.146$ 95% CI [0.0, 0.603]
[Block 1] NoVRS [Baseline] NoVRS	H(17) = 2.160 $p = 0.14164$	0.00985 0.01119	0.00120 0.00197	$\varepsilon^2 = 0.068$ 95% CI [0.0, 0.505]
[Block 2] VRS **[Block 2] NoVRS**	**H(18) = 10.080** $p = 0.00150$	**0.01054** **0.00841**	**0.00122** **0.00094**	$\varepsilon^2 = 0.504$ **95% CI [0.182, 0.752]**
[Block 2] VRS **[Baseline] VRS**	**H(16) = 8.084** $p = 0.00447$	**0.01054** **0.01313**	**0.00122** **0.00150**	$\varepsilon^2 = 0.443$ **95% CI [0.098, 0.742]**
[Block 2] NoVRS **[Baseline] NoVRS**	**H(18) = 10.566** $p = 0.00115$	**0.00841** **0.01119**	**0.00094** **0.00197**	$\varepsilon^2 = 0.531$ **95% CI [0.222, 0.746]**
[Block 3] VRS **[Block 3] NoVRS**	**H(18) = 7.406** $p = 0.00650$	**0.00958** **0.00790**	**0.00159** **0.00065**	$\varepsilon^2 = 0.356$ **95% CI [0.007, 0.748]**
[Block 3] VRS **[Baseline] VRS**	**H(16) = 9.126** $p = 0.00252$	**0.00958** **0.01313**	**0.00159** **0.00150**	$\varepsilon^2 = 0.508$ **95% CI [0.179, 0.741]**
[Block 3] NoVRS **[Baseline] NoVRS**	**H(18) = 12.623** $p = 0.00038$	**0.00790** **0.01119**	**0.00065** **0.00197**	$\varepsilon^2 = 0.646$ **95% CI [0.413, 0.748]**
[Block 4] VRS [Block 4] NoVRS	H(18) = 1.120 $p = 0.28992$	0.00774 0.00744	0.00072 0.00092	$\varepsilon^2 = 0.007$ 95% CI [0.0, 0.435]
[Block 4] VRS **[Baseline] VRS**	**H(16) = 12.632** $p = 0.00038$	**0.00774** **0.01313**	**0.00072** **0.00150**	$\varepsilon^2 = 0.727$ **95% CI [0.518, 0.742]**
[Block 4] NoVRS **[Baseline] NoVRS**	**H(18) = 13.720** $p = 0.00021$	**0.00744** **0.01119**	**0.00092** **0.00197**	$\varepsilon^2 = 0.707$ **95% CI [0.505, 0.753]**
[Block 5] VRS [Block 5] NoVRS	H(18) = 0.091 $p = 0.76237$	0.00737 0.00808	0.00069 0.00204	$\varepsilon^2 = 0.0$ 95% CI [0.0, 0.301]
[Block 5] VRS **[Baseline] VRS**	**H(16) = 12.632** $p = 0.00038$	**0.00737** **0.01313**	**0.00069** **0.00150**	$\varepsilon^2 = 0.727$ **95% CI [0.518, 0.743]**
[Block 5] NoVRS **[Baseline] NoVRS**	**H(18) = 9.606** $p = 0.00194$	**0.00808** **0.01119**	**0.00204** **0.00197**	$\varepsilon^2 = 0.478$ **95% CI [0.155, 0.748]**
[Block 6] VRS [Block 6] NoVRS	H(18) = 0.463 $p = 0.49629$	0.00779 0.00795	0.00114 0.00071	$\varepsilon^2 = 0.0$ 95% CI [0.0, 0.334]
[Block 6] VRS **[Baseline] VRS**	**H(16) = 12.632** $p = 0.00038$	**0.00779** **0.01313**	**0.00114** **0.00150**	$\varepsilon^2 = 0.727$ **95% CI [0.518, 0.741]**
[Block 6] NoVRS **[Baseline] NoVRS**	**H(18) = 12.091** $p = 0.00051$	**0.00795** **0.01119**	**0.00071** **0.00197**	$\varepsilon^2 = 0.616$ **95% CI [0.366, 0.753]**

Table 20: Vertical analysis results. Significant results ($p < 0.05$) are highlighted in bold.

Spatial Head Movement Forward				
Test	**Stats**	μ	σ	**Updated Effect Size**
[Baseline] VRS **[Baseline] NoVRS**	**H(16) = 12.632** $p = 0.00038$	**0.13691** **0.01119**	**0.04069** **0.00197**	$\varepsilon^2 = 0.727$ **95% CI [0.518, 0.743]**
[Block 1] VRS [Block 1] NoVRS	H(16) = 0.096 $p = 0.75728$	0.12045 0.12452	0.03174 0.05795	$\varepsilon^2 = 0.0$ 95% CI [0.0, 0.3]
[Block 1] VRS [Baseline] VRS	H(15) = 0.454 $p = 0.50058$	0.12045 0.13691	0.03174 0.04069	$\varepsilon^2 = 0.0$ 95% CI [0.0, 0.408]
[Block 1] NoVRS **[Baseline] NoVRS**	**H(17) = 13.500** $p = 0.00024$	**0.12452** **0.01119**	**0.05795** **0.00197**	$\varepsilon^2 = 0.750$ **95% CI [0.551, 0.750]**
[Block 2] VRS [Block 2] NoVRS	H(18) = 3.023 $p = 0.08210$	0.10171 0.08479	0.02395 0.02053	$\varepsilon^2 = 0.112$ 95% CI [0.0, 0.531]
[Block 2] VRS [Baseline] VRS	H(16) = 3.821 $p = 0.05061$	0.10171 0.13691	0.02395 0.04069	$\varepsilon^2 = 0.176$ 95% CI [0.0, 0.627]
[Block 2] NoVRS **[Baseline] NoVRS**	**H(18) = 14.286** $p = 0.00016$	**0.08479** **0.01119**	**0.02053** **0.00197**	$\varepsilon^2 = 0.738$ **95% CI [0.548, 0.755]**
[Block 3] VRS [Block 3] NoVRS	H(18) = 2.063 $p = 0.15093$	0.08865 0.07383	0.01601 0.03378	$\varepsilon^2 = 0.059$ 95% CI [0.0, 0.49]
[Block 3] VRS **[Baseline] VRS**	**H(16) = 9.671** $p = 0.00187$	**0.08865** **0.13691**	**0.01601** **0.04069**	$\varepsilon^2 = 0.542$ **95% CI [0.22, 0.741]**
[Block 3] NoVRS **[Baseline] NoVRS**	**H(18) = 14.286** $p = 0.00016$	**0.07383** **0.01119**	**0.03378** **0.00197**	$\varepsilon^2 = 0.738$ **95% CI [0.548, 0.755]**
[Block 4] VRS [Block 4] NoVRS	H(18) = 0.966 $p = 0.32575$	0.07535 0.06454	0.02106 0.01496	$\varepsilon^2 = 0.0$ 95% CI [0.0, 0.41]
[Block 4] VRS **[Baseline] VRS**	**H(16) = 10.808** $p = 0.00101$	**0.07535** **0.13691**	**0.02106** **0.04069**	$\varepsilon^2 = 0.613$ **95% CI [0.356, 0.742]**
[Block 4] NoVRS **[Baseline] NoVRS**	**H(18) = 14.286** $p = 0.00016$	**0.06454** **0.01119**	**0.01496** **0.00197**	$\varepsilon^2 = 0.738$ **95% CI [0.548, 0.755]**
[Block 5] VRS [Block 5] NoVRS	H(18) = 0.280 $p = 0.59670$	0.07329 0.07543	0.02509 0.01449	$\varepsilon^2 = 0.0$ 95% CI [0.0, 0.334]
[Block 5] VRS **[Baseline] VRS**	**H(16) = 9.671** $p = 0.00187$	**0.07329** **0.13691**	**0.02509** **0.04069**	$\varepsilon^2 = 0.542$ **95% CI [0.22, 0.741]**
[Block 5] NoVRS **[Baseline] NoVRS**	**H(18) = 14.286** $p = 0.00016$	**0.07543** **0.01119**	**0.01449** **0.00197**	$\varepsilon^2 = 0.738$ **95% CI [0.548, 0.755]**
[Block 6] VRS [Block 6] NoVRS	H(18) = 2.520 $p = 0.11241$	0.06343 0.08222	0.02360 0.02443	$\varepsilon^2 = 0.084$ 95% CI [0.0, 0.512]
[Block 6] VRS **[Baseline] VRS**	**H(16) = 11.400** $p = 0.00073$	**0.06343** **0.13691**	**0.02360** **0.04069**	$\varepsilon^2 = 0.650$ **95% CI [0.418, 0.743]**
[Block 6] NoVRS **[Baseline] NoVRS**	**H(18) = 14.286** $p = 0.00016$	**0.08222** **0.01119**	**0.02443** **0.00197**	$\varepsilon^2 = 0.738$ **95% CI [0.548, 0.755]**

Table 21: Forward analysis results. Significant results ($p < 0.05$) are highlighted in bold.

Temporal Head Movement Magnitude				
Test	**Stats**	μ	σ	**Updated Effect Size**
[Baseline] VRS [Baseline] NoVRS	H(16) = 1.547 $p = 0.21352$	1.72652 1.67493	0.04080 0.11064	$\varepsilon^2 = 0.034$ 95% CI [0.0, 0.483]
[Block 1] VRS [Block 1] NoVRS	H(16) = 0.096 $p = 0.75728$	1.75014 1.76849	0.11007 0.10866	$\varepsilon^2 = 0.0$ 95% CI [0.0, 0.284]
[Baseline] VRS [Block 1] VRS	H(15) = 1.565 $p = 0.21096$	1.72652 1.75014	0.04080 0.11007	$\varepsilon^2 = 0.038$ 95% CI [0.0, 0.535]
[Baseline] NoVRS [Block 1] NoVRS	H(17) = 3.227 $p = 0.07245$	1.67493 1.76849	0.11064 0.10866	$\varepsilon^2 = 0.131$ 95% CI [0.0, 0.606]
[Block 2] VRS **[Block 2] NoVRS**	**H(18) = 10.080** $p = 0.00150$	**1.75895** **1.63889**	**0.05858** **0.04453**	$\varepsilon^2 = 0.504$ **95% CI [0.114, 0.750]**
[Baseline] VRS [Block 2] VRS	H(16) = 3.158 $p = 0.07556$	1.72652 1.75895	0.04080 0.05858	$\varepsilon^2 = 0.135$ 95% CI [0.0, 0.620]
[Baseline] NoVRS [Block 2] NoVRS	H(18) = 2.063 $p = 0.15093$	1.67493 1.63889	0.11064 0.04453	$\varepsilon^2 = 0.059$ 95% CI [0.0, 0.564]
[Block 3] VRS **[Block 3] NoVRS**	**H(18) = 11.063** $p = 0.00088$	**1.73033** **1.61395**	**0.04084** **0.06126**	$\varepsilon^2 = 0.559$ **95% CI [0.214, 0.750]**
[Baseline] VRS [Block 3] VRS	H(16) = 0.008 $p = 0.92920$	1.72652 1.73033	0.04080 0.04084	$\varepsilon^2 = 0.0$ 95% CI [0.0, 0.274]
[Baseline] NoVRS [Block 3] NoVRS	H(18) = 2.063 $p = 0.15093$	1.67493 1.61395	0.11064 0.06126	$\varepsilon^2 = 0.059$ 95% CI [0.0, 0.536]
[Block 4] VRS **[Block 4] NoVRS**	**H(18) = 8.691** $p = 0.00320$	**1.71148** **1.61675**	**0.06049** **0.06016**	$\varepsilon^2 = 0.427$ **95% CI [0.086, 0.748]**
[Baseline] VRS [Block 4] VRS	H(16) = 0.032 $p = 0.85895$	1.72652 1.71148	0.04080 0.06049	$\varepsilon^2 = 0.0$ 95% CI [0.0, 0.277]
[Baseline] NoVRS [Block 4] NoVRS	H(18) = 3.291 $p = 0.06964$	1.67493 1.61675	0.11064 0.06016	$\varepsilon^2 = 0.127$ 95% CI [0.0, 0.654]
[Block 5] VRS **[Block 5] NoVRS**	**H(18) = 7.406** $p = 0.00650$	**1.71361** **1.64495**	**0.03834** **0.04735**	$\varepsilon^2 = 0.356$ **95% CI [0.027, 0.745]**
[Baseline] VRS [Block 5] VRS	H(16) = 0.387 $p = 0.53396$	1.72652 1.71361	0.04080 0.03834	$\varepsilon^2 = 0.0$ 95% CI [0.0, 0.330]
[Baseline] NoVRS [Block 5] NoVRS	H(18) = 1.286 $p = 0.25684$	1.67493 1.64495	0.11064 0.04735	$\varepsilon^2 = 0.016$ 95% CI [0.0, 0.481]
[Block 6] VRS [Block 6] NoVRS	H(18) = 0.091 $p = 0.76237$	1.68462 1.67629	0.06353 0.08828	$\varepsilon^2 = 0.0$ 95% CI [0.0, 0.254]
[Baseline] VRS [Block 6] VRS	H(16) = 2.021 $p = 0.15513$	1.72652 1.68462	0.04080 0.06353	$\varepsilon^2 = 0.064$ 95% CI [0.0, 0.547]
[Baseline] NoVRS [Block 6] NoVRS	H(18) = 0.143 $p = 0.70546$	1.67493 1.67629	0.11064 0.08828	$\varepsilon^2 = 0.0$ 95% CI [0.0, 0.273]

Table 22: Magnitude analysis results. Significant results ($p < 0.05$) are highlighted in bold.

Spatial Head Movement Lateral				
Test	**Stats**	μ	σ	**Updated Effect Size**
[Baseline] VRS [Baseline] NoVRS	H(16) = 0.032 $p = 0.85895$	1.70384 1.71497	0.02815 0.11074	$\varepsilon^2 = 0.0$ 95% CI [0.0, 0.28]
[Block 1] VRS [Block 1] NoVRS	H(16) = 0.439 $p = 0.50780$	1.69826 1.72000	0.08858 0.10944	$\varepsilon^2 = 0.0$ 95% CI [0.0, 0.354]
[Baseline] VRS [Block 1] VRS	H(15) = 0.037 $p = 0.84739$	1.70384 1.69826	0.02815 0.08858	$\varepsilon^2 = 0.0$ 95% CI [0.0, 0.288]
[Baseline] NoVRS [Block 1] NoVRS	H(17) = 0.240 $p = 0.62421$	1.71497 1.72000	0.11074 0.10944	$\varepsilon^2 = 0.0$ 95% CI [0.0, 0.301]
[Block 2] VRS **[Block 2] NoVRS**	**H(18) = 5.851** $p = 0.01556$	**1.67018** **1.58738**	**0.07111** **0.04694**	$\varepsilon^2 = 0.270$ **95% CI [0.0, 0.741]**
[Baseline] VRS [Block 2] VRS	H(16) = 0.639 $p = 0.42390$	1.70384 1.67018	0.02815 0.07111	$\varepsilon^2 = 0.0$ 95% CI [0.0, 0.375]
[Baseline] NoVRS **[Block 2] NoVRS**	**H(18) = 8.251** $p = 0.00407$	**1.71497** **1.58738**	**0.11074** **0.04694**	$\varepsilon^2 = 0.403$ **95% CI [0.049, 0.750]**
[Block 3] VRS **[Block 3] NoVRS**	**H(18) = 14.286** $p = 0.00016$	**1.67075** **1.57216**	**0.04286** **0.04557**	$\varepsilon^2 = 0.738$ **95% CI [0.380, 0.750]**
[Baseline] VRS [Block 3] VRS	H(16) = 3.482 $p = 0.06206$	1.70384 1.67075	0.02815 0.04286	$\varepsilon^2 = 0.155$ 95% CI [0.0, 0.636]
[Baseline] NoVRS **[Block 3] NoVRS**	**H(18) = 9.606** $p = 0.00194$	**1.71497** **1.57216**	**0.11074** **0.04557**	$\varepsilon^2 = 0.478$ **95% CI [0.089, 0.750]**
[Block 4] VRS **[Block 4] NoVRS**	**H(18) = 9.606** $p = 0.00194$	**1.65422** **1.55941**	**0.06091** **0.04809**	$\varepsilon^2 = 0.478$ **95% CI [0.075, 0.750]**
[Baseline] VRS [Block 4] VRS	H(16) = 2.558 $p = 0.10974$	1.70384 1.65422	0.02815 0.06091	$\varepsilon^2 = 0.097$ 95% CI [0.0, 0.589]
[Baseline] NoVRS **[Block 4] NoVRS**	**H(18) = 9.606** $p = 0.00194$	**1.71497** **1.55941**	**0.11074** **0.04809**	$\varepsilon^2 = 0.478$ **95% CI [0.083, 0.750]**
[Block 5] VRS **[Block 5] NoVRS**	**H(18) = 8.251** $p = 0.00407$	**1.63998** **1.53606**	**0.06842** **0.02893**	$\varepsilon^2 = 0.403$ **95% CI [0.0, 0.743]**
[Baseline] VRS **[Block 5] VRS**	**H(16) = 6.189** $p = 0.01285$	**1.70384** **1.63998**	**0.02815** **0.06842**	$\varepsilon^2 = 0.324$ **95% CI [0.0, 0.741]**
[Baseline] NoVRS **[Block 5] NoVRS**	**H(18) = 9.143** $p = 0.00250$	**1.71497** **1.53606**	**0.11074** **0.02893**	$\varepsilon^2 = 0.452$ **95% CI [0.093, 0.749]**
[Block 6] VRS [Block 6] NoVRS	H(18) = 2.063 $p = 0.15093$	1.64032 1.59697	0.05811 0.08101	$\varepsilon^2 = 0.059$ 95% CI [0.0, 0.547]
[Baseline] VRS **[Block 6] VRS**	**H(16) = 6.189** $p = 0.01285$	**1.70384** **1.64032**	**0.02815** **0.05811**	$\varepsilon^2 = 0.324$ **95% CI [0.0, 0.738]**
[Baseline] NoVRS **[Block 6] NoVRS**	**H(18) = 5.851** $p = 0.01556$	**1.71497** **1.59697**	**0.11074** **0.08101**	$\varepsilon^2 = 0.270$ **95% CI [0.0, 0.741]**

Table 23: Lateral analysis results. Significant results ($p < 0.05$) are highlighted in bold.

Spatial Head Movement Vertical				
Test	**Stats**	μ	σ	**Updated Effect Size**
[Baseline] VRS [Baseline] NoVRS	H(16) = 0.032 $p = 0.85895$	1.14651 1.12610	0.06124 0.14354	$\varepsilon^2 = 0.0$ 95% CI [0.0, 0.28]
[Block 1] VRS [Block 1] NoVRS	H(16) = 0.002 $p = 0.96478$	1.03052 1.03973	0.07373 0.04880	$\varepsilon^2 = 0.0$ 95% CI [0.0, 0.231]
[Baseline] VRS **[Block 1] VRS**	**H(15) = 7.259** $p = 0.00705$	**1.14651** **1.03052**	**0.06124** **0.07373**	$\varepsilon^2 = 0.417$ **95% CI [0.0, 0.741]**
[Baseline] NoVRS [Block 1] NoVRS	H(17) = 2.160 $p = 0.14164$	1.12610 1.03973	0.14354 0.04880	$\varepsilon^2 = 0.073$ 95% CI [0.0, 0.518]
[Block 2] VRS **[Block 2] NoVRS**	**H(18) = 3.863** $p = 0.04937$	**1.10482** **1.03047**	**0.07789** **0.06358**	$\varepsilon^2 = 0.159$ **95% CI [0.0, 0.702]**
[Baseline] VRS [Block 2] VRS	H(16) = 1.334 $p = 0.24806$	1.14651 1.10482	0.06124 0.07789	$\varepsilon^2 = 0.021$ 95% CI [0.0, 0.443]
[Baseline] NoVRS [Block 2] NoVRS	H(18) = 2.766 $p = 0.09630$	1.12610 1.03047	0.14354 0.06358	$\varepsilon^2 = 0.098$ 95% CI [0.0, 0.569]
[Block 3] VRS **[Block 3] NoVRS**	**H(18) = 6.606** $p = 0.01017$	**1.14433** **1.03664**	**0.06897** **0.06223**	$\varepsilon^2 = 0.311$ **95% CI [0.0, 0.744]**
[Baseline] VRS [Block 3] VRS	H(16) = 0.000 $p = 1.00000$	1.14651 1.14433	0.06124 0.06897	$\varepsilon^2 = 0.0$ 95% CI [0.0, 0.134]
[Baseline] NoVRS [Block 3] NoVRS	H(18) = 3.291 $p = 0.06964$	1.12610 1.03664	0.14354 0.06223	$\varepsilon^2 = 0.127$ 95% CI [0.0, 0.612]
[Block 4] VRS [Block 4] NoVRS	H(18) = 1.651 $p = 0.19876$	1.08900 1.05706	0.04719 0.05481	$\varepsilon^2 = 0.036$ 95% CI [0.0, 0.491]
[Baseline] VRS [Block 4] VRS	H(16) = 3.821 $p = 0.05061$	1.14651 1.08900	0.06124 0.04719	$\varepsilon^2 = 0.176$ 95% CI [0.0, 0.655]
[Baseline] NoVRS [Block 4] NoVRS	H(18) = 2.063 $p = 0.15093$	1.12610 1.05706	0.14354 0.05481	$\varepsilon^2 = 0.059$ 95% CI [0.0, 0.548]
[Block 5] VRS **[Block 5] NoVRS**	**H(18) = 4.480** $p = 0.03429$	**1.11153** **1.02672**	**0.08296** **0.05873**	$\varepsilon^2 = 0.193$ **95% CI [0.0, 0.713]**
[Baseline] VRS [Block 5] VRS	H(16) = 1.137 $p = 0.28632$	1.14651 1.11153	0.06124 0.08296	$\varepsilon^2 = 0.009$ 95% CI [0.0, 0.413]
[Baseline] NoVRS [Block 5] NoVRS	H(18) = 3.291 $p = 0.06964$	1.12610 1.02672	0.14354 0.05873	$\varepsilon^2 = 0.127$ 95% CI [0.0, 0.643]
[Block 6] VRS [Block 6] NoVRS	H(18) = 0.571 $p = 0.44969$	1.10124 1.10450	0.04882 0.06104	$\varepsilon^2 = 0.0$ 95% CI [0.0, 0.354]
[Baseline] VRS [Block 6] VRS	H(16) = 1.776 $p = 0.18260$	1.14651 1.10124	0.06124 0.04882	$\varepsilon^2 = 0.049$ 95% CI [0.0, 0.518]
[Baseline] NoVRS [Block 6] NoVRS	H(18) = 1.286 $p = 0.25684$	1.12610 1.10450	0.14354 0.06104	$\varepsilon^2 = 0.016$ 95% CI [0.0, 0.468]

Table 24: Vertical analysis results. Significant results ($p < 0.05$) are highlighted in bold.

Spatial Head Movement Forward				
Test	**Stats**	μ	σ	**Updated Effect Size**
[Baseline] VRS [Baseline] NoVRS	H(16) = 0.126 $p = 0.72228$	1.76631 1.74658	0.05244 0.10594	$\varepsilon^2 = 0.0$ 95% CI [0.0, 0.306]
[Block 1] VRS [Block 1] NoVRS	H(16) = 0.018 $p = 0.89463$	1.79466 1.79768	0.08089 0.08036	$\varepsilon^2 = 0.0$ 95% CI [0.0, 0.231]
[Baseline] VRS [Block 1] VRS	H(15) = 1.815 $p = 0.17793$	1.76631 1.79466	0.05244 0.08089	$\varepsilon^2 = 0.054$ 95% CI [0.0, 0.556]
[Baseline] NoVRS [Block 1] NoVRS	H(17) = 1.127 $p = 0.28849$	1.74658 1.79768	0.10594 0.08036	$\varepsilon^2 = 0.007$ 95% CI [0.0, 0.446]
[Block 2] VRS **[Block 2] NoVRS**	**H(18) = 6.606** $p = 0.01017$	**1.78589** **1.70633**	**0.05677** **0.05521**	$\varepsilon^2 = 0.311$ **95% CI [0.0, 0.744]**
[Baseline] VRS [Block 2] VRS	H(16) = 0.505 $p = 0.47720$	1.76631 1.78589	0.05244 0.05677	$\varepsilon^2 = 0.0$ 95% CI [0.0, 0.364]
[Baseline] NoVRS [Block 2] NoVRS	H(18) = 2.766 $p = 0.09630$	1.74658 1.70633	0.10594 0.05521	$\varepsilon^2 = 0.098$ 95% CI [0.0, 0.584]
[Block 3] VRS **[Block 3] NoVRS**	**t(18) = 2.543** $p = 0.02041$	**1.77755** **1.70574**	**0.04105** **0.07411**	$\varepsilon^2 = 0.311$ **95% CI [0.0, 0.743]**
[Baseline] VRS [Block 3] VRS	H(16) = 0.197 $p = 0.65685$	1.76631 1.77755	0.05244 0.04105	$\varepsilon^2 = 0.0$ 95% CI [0.0, 0.311]
[Baseline] NoVRS [Block 3] NoVRS	H(18) = 2.766 $p = 0.09630$	1.74658 1.70574	0.10594 0.07411	$\varepsilon^2 = 0.098$ 95% CI [0.0, 0.569]
[Block 4] VRS [Block 4] NoVRS	H(18) = 2.063 $p = 0.15093$	1.75105 1.70827	0.05368 0.05396	$\varepsilon^2 = 0.059$ 95% CI [0.0, 0.536]
[Baseline] VRS [Block 4] VRS	H(16) = 0.387 $p = 0.53396$	1.76631 1.75105	0.05244 0.05368	$\varepsilon^2 = 0.0$ 95% CI [0.0, 0.344]
[Baseline] NoVRS [Block 4] NoVRS	H(18) = 3.023 $p = 0.08210$	1.74658 1.70827	0.10594 0.05396	$\varepsilon^2 = 0.112$ 95% CI [0.0, 0.602]
[Block 5] VRS **[Block 5] NoVRS**	**H(18) = 8.251** $p = 0.00407$	**1.74338** **1.66282**	**0.05419** **0.04156**	$\varepsilon^2 = 0.403$ **95% CI [0.038, 0.750]**
[Baseline] VRS [Block 5] VRS	H(16) = 1.547 $p = 0.21352$	1.76631 1.74338	0.05244 0.05419	$\varepsilon^2 = 0.034$ 95% CI [0.0, 0.499]
[Baseline] NoVRS **[Block 5] NoVRS**	**H(18) = 7.823** $p = 0.00516$	**1.74658** **1.66282**	**0.10594** **0.04156**	$\varepsilon^2 = 0.379$ **95% CI [0.021, 0.748]**
[Block 6] VRS [Block 6] NoVRS	H(18) = 0.280 $p = 0.59670$	1.71008 1.70484	0.04440 0.08245	$\varepsilon^2 = 0.0$ 95% CI [0.0, 0.301]
[Baseline] VRS **[Block 6] VRS**	**H(16) = 4.934** $p = 0.02633$	**1.76631** **1.71008**	**0.05244** **0.04440**	$\varepsilon^2 = 0.246$ **95% CI [0.0, 0.735]**
[Baseline] NoVRS [Block 6] NoVRS	H(18) = 1.851 $p = 0.17362$	1.74658 1.70484	0.10594 0.08245	$\varepsilon^2 = 0.047$ 95% CI [0.0, 0.531]

Table 25: Forward analysis results. Significant results ($p < 0.05$) are highlighted in bold.

Table 31: Experimental (VR Walking) models: meanPool results for AP and F1-score (mean ± sd).

Model	Source	AP	F1-score
logistic_e	All	0.57 ± 0.20	0.44 ± 0.32
logistic_e	CoM	0.51 ± 0.11	0.54 ± 0.38
logistic_e	Head	0.71 ± 0.24	0.48 ± 0.36
logistic_e_alpha_only	All	0.46 ± 0.11	0.44 ± 0.31
logistic_e_alpha_only	CoM	0.69 ± 0.24	0.56 ± 0.42
logistic_e_alpha_only	Head	0.56 ± 0.07	0.49 ± 0.07
logistic_e_spatial_only	All	0.79 ± 0.15	0.53 ± 0.19
logistic_e_spatial_only	CoM	0.78 ± 0.21	0.53 ± 0.38
logistic_e_spatial_only	Head	0.59 ± 0.15	0.47 ± 0.05

Table 32: Experimental (VR Walking) models: LSE results for ACC and AUC (mean ± sd).

Model	Source	ACC	AUC
logistic_e	All	0.42 ± 0.19	0.28 ± 0.28
logistic_e	CoM	0.54 ± 0.26	0.33 ± 0.24
logistic_e	Head	0.61 ± 0.18	0.56 ± 0.32
logistic_e_alpha_only	All	0.50 ± 0.09	0.43 ± 0.00
logistic_e_alpha_only	CoM	0.60 ± 0.33	0.61 ± 0.28
logistic_e_alpha_only	Head	0.38 ± 0.03	0.46 ± 0.18
logistic_e_spatial_only	All	0.63 ± 0.26	0.74 ± 0.19
logistic_e_spatial_only	CoM	0.64 ± 0.22	0.72 ± 0.28
logistic_e_spatial_only	Head	0.44 ± 0.11	0.28 ± 0.21

Table 33: Experimental (VR Walking) models: LSE results for AP and F1-score (mean ± sd).

Model	Source	AP	F1-score
logistic_e	All	0.54 ± 0.18	0.44 ± 0.32
logistic_e	CoM	0.51 ± 0.11	0.54 ± 0.38
logistic_e	Head	0.71 ± 0.24	0.48 ± 0.36
logistic_e_alpha_only	All	0.51 ± 0.06	0.58 ± 0.13
logistic_e_alpha_only	CoM	0.69 ± 0.24	0.56 ± 0.42
logistic_e_alpha_only	Head	0.56 ± 0.07	0.49 ± 0.07
logistic_e_spatial_only	All	0.82 ± 0.12	0.66 ± 0.25
logistic_e_spatial_only	CoM	0.78 ± 0.21	0.53 ± 0.38
logistic_e_spatial_only	Head	0.59 ± 0.15	0.47 ± 0.05

Table 34: Axis-level SHAP importances (mean absolute contributions) for logistic_b.

Source	AnteriorPosterior	Lateral	Magnitude	UPDown
All	0.138	0.284	0.247	0.331
CoM	0.113	0.261	0.196	0.430
Head	0.394	0.286	0.085	0.235

Table 35: Axis-level SHAP importances (mean absolute contributions) for logistic_b_alpha_only.

Source	AnteriorPosterior	Lateral	Magnitude	UPDown
All	0.359	0.224	0.373	0.044
CoM	0.079	0.390	0.275	0.257
Head	0.524	0.137	0.292	0.047

Table 36: Axis-level SHAP importances (mean absolute contributions) for logistic_b_spatial_only.

Source	AnteriorPosterior	Lateral	Magnitude	UPDown
All	0.177	0.250	0.237	0.337
CoM	0.102	0.230	0.224	0.444
Head	0.300	0.362	0.134	0.205

Table 37: Axis-level SHAP importances (mean absolute contributions) for logistic_e.

Source	AnteriorPosterior	Lateral	Magnitude	UPDown
All	0.152	0.302	0.267	0.279
CoM	0.191	0.330	0.208	0.271
Head	0.246	0.289	0.255	0.210

Table 38: Axis-level SHAP importances (mean absolute contributions) for logistic_e_alpha_only.

Source	AnteriorPosterior	Lateral	Magnitude	UPDown
All	0.076	0.525	0.117	0.282
CoM	0.049	0.766	0.112	0.072
Head	0.168	0.098	0.176	0.559

Table 39: Axis-level SHAP importances (mean absolute contributions) for logistic_e_spatial_only.

Source	AnteriorPosterior	Lateral	Magnitude	UPDown
All	0.177	0.250	0.237	0.337
CoM	0.102	0.230	0.224	0.444
Head	0.300	0.362	0.134	0.205